SISSA - SCUOLA
INTERNAZIONALE
SUPERIORE
DI STUDI AVANZATI
TRIESTE
Strada Costiera 11

ISAS - INTERNATIONAL SCHOOL FOR ADVANCED STUDIES

October 1984

GALAXY FORMATION AND GLOBULAR CLUSTERS

Thesis submitted for the degree

of

Master of Philosophy

CANDIDATE:

Manorama S.

SUPERVISOR:

Prof.D.W.Sciama

TRIESTE

ISAS - INTERNATIONAL SCHOOL FOR ADVANCED STUDIES

October 1984

GALAXY FORMATION AND GLOBULAR CLUSTERS

Thesis submitted for the degree

of

Master of Philosophy

CANDIDATE:

Manorama S.

SUPERVISOR:

Prof.D.W.Sciama

CONTENTS

	Introduction	
I	THE LARGE SCALE STRUCTURE	1
1.1	The Standard Model	1
1.2	The Density of Matter in the Universe	5
1.3	The Dark Matter	10
1.4	The Distribution of Matter in the Universe	14
II	THE GROWTH OF STRUCTURE IN THE UNIVERSE	21
2.1	Gravitational Instability	21
2.2	The Density Perturbations	25
2.3	The Fluctuation Spectrum	27
2.4	The Types of Fluctuations	29
2.5	Galaxy Formation	32
III	GALAXY FORMATION WITH DARK MATTER	36
3.1	Hot,Warm and Cold Dark Matter	37
3.2	Galaxy Formation with Hot DM	38
3.3	Galaxy Formation with Warm DM	48
3.4	Galaxy Formation with Cold DM	50
IV	THE GLOBULAR CLUSTERS	57
4.1	Dark Matter and Globular Clusters	58
4.2	Globular Clusters with Massive Halos	60
4.3	Tests for Massive Halos in Globular Clusters	60

INTRODUCTION

The universe is homogenous and isotropic only in an average sense and only on the very largest scales. Galaxies, clusters of galaxies and superclusters represent inhomogenities on scales as large as 20 to 100 MPC. The existence of these inhomogenities implies that the early universe must have contained fluctuations in the density of matter. Overdense regions would then expand more slowly than the background and eventually, provided the fluctuations were not damped, they would stop expanding and collapse to form bound objects. To understand how galaxies form we need to know how the initial density fluctuations arise, under what circumstances they evolve into bound objects and how the bound objects develop the observed characteristics we see today.

Primordial density fluctuations can, in principle, occur in two forms: (i) isothermal perturbations and (ii) adiabatic perturbations. Though in principle both are allowed , grand unified theories of the strong, weak and electromagnetic interactions actually force us to consider only adiabatic perturbations. With purely adiabatic perturbations present in a baryon-dominated universe, the first structures to form are of the scales of superclusters($10^{15} - 10^{16}\ M_\odot$). The galaxy formation takes place by the fragmentation of these protoclusters. This scenario, popularly called the "top-down" model of galaxy formation, has difficulties to reconcile with observations of the microwave background, and the spatial distribution of galaxies, unless the cosmological density $\Omega = 1$. But $\Omega \approx 1$ baryon-dominated universe is in conflict with the upper limits on the baryon density($\Omega \leq 0.1$) inferred from big bang nucleosynthesis arguments concerning the abundance of He, D and ^{7}Li. On the other hand, however, evidence based upon dynamical arguments suggest that $\Omega \sim 1$, implying the existence of dark matter.

The nature of this dark matter is still an unsolved problem. But if it is the dominant matter in the universe, it is likely that it plays an important role in galaxy formation. Recent developments in particle physics, have given a long list of candidates , whose relic abundance could supply the mass density contributed by dark matter. These candidates are classified as hot, warm and cold dark matter, according to their initial random velocities relative to the comoving expanding frame of the universe.

The role of these particles in the formation of structures in the universe is discussed here and it is shown that the hot and warm dark matter scenarios for

galaxy formation are not compatible with observations. The cold dark matter picture seems to be the more promising. In this scenario the first objects to form are globular clusters. These globular clusters are formed with massive halos around them. At present, there is no direct observational evidence to show that globular clusters do have dark matter halos. Some of the properties of globular clusters , in the light of the cold dark matter model, are discussed here. We also comment on possible observational tests to detect the massive halos of globular clusters.

CHAPTER ONE
THE LARGE SCALE STRUCTURE

1.1 THE STANDARD MODEL

The appropriate framework to describe the universe seems to be the Standard Big Bang model.The Big Bang model is based on the Cosmological principle and the theory of general relativity. The Cosmological principle is the hypothesis that the universe is spatially homogeneous and isotropic so that it appears the same in any direction or from any spot.The general relativity theory ensures that the laws of physics are the same everywhere in space and do not change with time.Accumulating observational evidence over the past fifty years supports the standard model. The Hubble expansion, the existence of the 2.7°K cosmic background radiation with its characteristic blackbody spectrum and near perfect isotropy,the accurate determination of the light elements (D, ^3He, ^7Li)that is,the primordial nucleosynthesis,may all be considered as evidences for the standard picture.Now it is generally accepted that the standard model gives an accurate accounting of the history of the universe from about $\sim 10^{-2}$ seconds seconds after the "bang" when the temperature was about 10 Mev,until today,some 10-20 billion years after the "bang" with temperature of about 2.7°K($\approx 3 \times 10^{-13}$ Gev). Extending our understanding further back to earlier times and higher temperatures requires knowledge about the fundamental particles and their interactions at very high energies. And prior to 10^{-43} seconds,the Planck time,gravity needs to be quantised and the subject is still not very developed atthe moment.

Observations indicate that on the largest scales(>> 100 MPC),the universe is isotropic and homogeneous and it can be accurately described by the Robertson-Walker metric (Weinberg 1972)

$$ds^2 = dt^2 - R^2(t)\left[\frac{dr^2}{1-kr^2} + r^2 d\theta^2 + r^2 \sin^2\theta\, d\phi^2\right] \qquad (1.1)$$

where ds^2 is the proper separation between two events,(r, θ, ϕ, t)represents the space-time coordinates , R(t) is the cosmic scale factor and $k = +1,0,-1$ is the curvature signature which indicates the type of universe we live in; closed,flat,or open respectively.

The dynamical evolution of such a universe is given by combining eqn.(1.1) with Einstein's field equations.Taking the Cosmological Constant Λ =0, we get (Friedmann's equations)

$$H^2 \equiv \left(\frac{\dot{R}}{R}\right)^2 = \frac{8}{3}\pi G\rho - \frac{k}{R^2} \qquad (1.2)$$

where $H \equiv \dot{R}/R$ is the Hubble constant which gives the expansion rate of the universe and ρ is the total energy density in the universe.

Energy conservation relates the density ρ to the pressure p and this is expressed by

$$\frac{d}{dR}(\rho R^3) = -3pR^2 \qquad (1.3)$$

Solving this equation requires an equation of state $p = p(\rho)$ for the medium. If the density of the universe is dominated by non-relativistic matter, "dust", the pressure can be neglected . Then eqn.(1.3) gives

$$\rho \propto R^{-3} \quad \text{for} \quad p = 0 \qquad (1.4)$$

In the early phase of the universe,the energy density was dominated by photons and using the equation of state for relativistic particles, eqn.(1.3) gives

$$\rho \propto R^{-4} \quad \text{for} \quad p = \frac{1}{3}\rho c^2 \qquad (1.5)$$

In general,with a perfect fluid equation of state $p = (\gamma-1)\rho, \ (1 \le \gamma \le 2)$ we get

$$\rho \propto R^{-3\gamma} \qquad (1.6)$$

Knowing ρ as a function of R, we can determine the cosmic factor R(t) for all time by solving eqn.(1.2).

It is useful to have a number of parameters that quantify the observed expansion of the universe.

The Hubble constant H.

The present value of the Hubble constant H_0 is observed to lie in the range

$$H_0 = 75 \pm 25 \ km\, s^{-1} Mpc^{-1} \tag{1.7}$$

The subscript zero denotes the present epoch. The Hubble parameter is usually expressed in the dimensionless form

$$h_0 = H_0 / 100 \ km\, s^{-1} Mpc^{-1} \tag{1.8}$$

The density parameter ρ

The density parameter ρ of the universe is expressed in units of the critical density ρ_c. It is the largest density the universe can possess and expand for all future time. It is given by

$$\rho_c \equiv 3H_0^2 / 8\pi G \sim 2 \times 10^{-29} h_0^2 \ gm\, cm^{-3} \tag{1.9}$$

The density in the universe is then expressed as the ratio

$$\Omega = \rho / \rho_c \tag{1.10}$$

Ω is called the Cosmological density parameter. The determination of its value is one of the primary goals of observational cosmology.
If $\Omega > 1$ the universe will eventually recollapse while $\Omega \leq 1$ implies that it is going to continue expanding forever. At present, Ω is known only to lie in the range $0.014 < \Omega < 3$. The lower limit comes from the primordial nucleosynthesis argument $(\Omega \geq \Omega_b \geq 0.014)$ and the upper limit from the age of the universe(Yang et.al 1984; Zeldovich et.al. 1979), $(\Omega \leq 3)$.

Age of the universe t_U

The parameters H and Ω can be used to determine the age of the universe . This is given by the relation(Weinberg 1972)

$$t_U = \frac{f(\Omega)}{H} \qquad (1.11)$$

where $f(\Omega)$ is a monotonic function.For the three models of the universe, closed,flat or open, this function is given as

$$f(\Omega) = \frac{\Omega}{2(\Omega-1)^{3/2}}\left[\cos^{-1}\left(\frac{2}{\Omega}-1\right) - \frac{2}{\Omega}(\Omega-1)^{1/2}\right] \quad \text{for } \Omega>1$$

$$f(\Omega) = \frac{2}{3} \quad \text{for } \Omega = 1$$

$$f(\Omega) = (1-\Omega)^{-1} - \frac{\Omega}{2}(1-\Omega)^{-3/2}\cosh^{-1}\left(\frac{2}{\Omega}-1\right) \quad \text{for } \Omega<1$$

From the observational data on the oldest stars present in the globular clusters in the Galaxy and from the age of the Galaxy supplied by $^{237}Th/^{238}U$ and $^{187}Re/^{183}Os$ the age of the universe is found to be(Audouze 1979, Symbalisty and Schramm 1981)

$$13.5\times10^9 \text{ years} < t_U < 20\times10^9 \text{ years} \qquad (1.13)$$

The uncertainities are those which come from the poorly known H_0 and Ω.

There are two cosmological epochs of interest for us.Recombination and the epoch of equal matter and radiation density.

Recombination occurs when the radiation temperature drops to $\sim 3000\,^{\circ}K$ and the protons and electrons combine to hydrogen. Given the present temperature of 2.7°K this occurs at a redshift $(1+z_r)\sim 10^3$ for all values of Ω between 0.1 and 1.0.

The epoch of equal matter and radiation occurs at

$(1+z_{eq})\sim 10^4$ for $\Omega = 1$

$(1+z_{eq})\sim 10^3$ for $\Omega = 0.1$

1.2 THE DENSITY OF MATTER IN THE UNIVERSE

One of the fundamental cosmological quantities is the mean mass density ρ of the universe. DIscussion of ρ is particularly difficult because for every conceivable form of matter in the universe, we have to find from observations and theory, an estimate of the amount or an upper limit to the mass. We have seen that ρ can be expressed in terms of Ω (eqn.1.10). There is no strong observational evidence that ρ should equal the critical density, ρ_c.

A way to measure Ω on very large scales is to determine the deceleration parameter q_0. The deceleration parameter is given by(Weinberg 1972)

$$q_0 = -\left(\frac{\ddot{R}R}{\dot{R}^2}\right)_0$$

For $\Lambda = 0$, we get from eqn.(1.2), $\Omega = 2q_0$.
Once q_0 is determined we can get Ω. Although q_0 in principle be measured from the deviation of very distant objects from Hubble's law, the difficulty lies in knowing the true distance of these objects.The estimates should take into consideration the evolution and sampling effects of these objects. Observations indicate a range of q_0 from 0 ± 0.5 to 1.5 ± 0.5(Sandage and Hardy 1973, Tammann et.al. 1979). This gives an upper limit to $\Omega \leq 4$. The age of universe gives an upper limit to the value of Ω. In a Friedmann universe, a larger value of Ω implies a younger universe. From the age of the universe (see eqn.1.13) we get $\Omega \leq 3.2$.

There is no strong observational evidence for ρ to ρ_c so, $\Omega = 1$.
But there is also no guarantee that all the significant contributions to the mean mass density will be in the forms that can be detected by us. In fact, we will see that there is enough observational evidence for the existence of a kind of matter, the dark matter (DM) or popularly known as the missing mass, dominating the total mass in the universe. This DM is detected through its gravitational attraction in the massive extended halos of spiral galaxies and in groups and clusters of galaxies of all sizes. This matter is appropriately called " dark " because it is detected in no other way;it is not observed to emit or absorb eletromagnetic radiation of any wavelength.

From a theorist's point of view, the determination of ρ, the mean mass density in the universe is all straightforward:

$$\rho = n_{gal} \times M_{gal} \qquad (1.14)$$

That is, one determines the number density of galaxies n_{gal} and multiplies it by the mass associated with a galaxy M_{gal}, assuming that light faithfully follows mass. The oldest method and still the most widely used one for measuring ρ, is the mass-to-light technique. In this method, one determines the average M/L ratio associated with an object and multiplying it by the luminosity density, one gets the ρ associated with that object.That is,

$$\rho = \mathcal{L}\left(\frac{M}{L}\right) \tag{1.15}$$

The luminosity density $\mathcal{L}$ is a readily measured observational quantity.
Note that is assumed even here that the luminosity is a "tracer" of the mass.All the calculations are based on this assumption, a highly non- trivial one. Since our knowledge of the universe is derived primarily from light (the photons), it is difficult to find a method which does not rely on this assumption.

The mean luminosity density of the universe is obtained from the luminosity function of galaxies. A galaxy luminosity function, $\phi(L)dL$, is defined so that it gives the number of galaxies per unit volume, with luminosities between L and $L+dL$. Schechter (1976) has shown that the luminosity function of galaxies in rich clusters is best fitted by the expression

$$\phi(L)dL = \phi^*\left(\frac{L}{L^*}\right)^{\alpha} exp\left(\frac{-L}{L^*}\right)dL \tag{1.16}$$

where L, ϕ^* are constants and L^* is the luminosity corresponding to a B(0) absolute magnitude of -20.6. Efstathiou et al. (1983) gave the values of L and ϕ^* as

$$\alpha = -1.29 \pm 0.11$$

$$\phi^* = 1.3 \pm 0.3 \times 10^{2} h_0^3 MPc^{-3}$$

With these values the mean luminosity density of the universe is

$$\mathcal{L} \sim 1.9 \times 10^{8} h_0 \left(L_\odot MPc^{-3}\right) \tag{1.17}$$

Corresponding to this $\mathcal{L}$ we can define a critcal $(M/L)_c$ ratio as

$$\left(\frac{M}{L}\right)_c \equiv \frac{\rho_c}{\mathcal{L}} \approx 1.4 \times 10^3 h_0 \left(\frac{M_\odot}{L_\odot}\right) \qquad (1.18)$$

The mass-to-light ratios from observations, of the different objects in the universe is given in Table 1 (Faber and Gallagher 1979).The most striking fact from this data is that the observed mass-to-light ratios seems to be increasing with scale from the $M/L \sim (1-2)$ for the Solar neighborhood to $M/L \sim (400-600)h_0$ for rich clusters.This implies that there is a considerable amount of mass in large systems that is non-luminous, "dark". Figure 1 shows the observed mass-to-light ratios as a function of the measuring scale. From this figure Davis et.al. suggested that the M/L versus scale might be approaching an asymptotic limit (perhaps $\Omega = 1$) on the scales of superclusters. Gott and Turner (1977) believe that the curve flattens already on the scales of binary galaxies and small groups of galaxies. However, what is significant from these measurements is that there is more matter in the universe which is dark and increases with scale.

It has become clear in the past decade that, not only is there a great deal of DM in rich clusters but that there is dark matter associated with individual galaxies as well.The strongest evidence for this comes from the studies of the rotational velocity V versus radius γ in the disks of Spiral galaxies.(Faber and Gallagher 1979 V.C.Rubin et.al.1982 , Burstein et.al. 1982). From the application of simple newtonian mechanics to a system in equilibrium, it is found that Spiral galaxies are surrounded by a large amount of dark matter.

The technique by which the mass of a distant object is measured relies upon Kepler's third law:

$$GM = \gamma \times V^2 \qquad (1.19)$$

where γ and V are the orbital radius and velocity of a test object(say,gas) which orbits the mass M . The mass associated with a galaxy can be determined by studying the orbits of stars and gas clouds at the distance from its center where the light falls off-the Holmberg radius γ_H . The Holmberg radius is defined as the radius at which the surface brightness of an object reaches an apparent mag. 26.7mag/sq.arc sec. It is a convenient measure of the optical extent of a galaxy. For a spiral galaxy, $\gamma_H \sim 10-30$ kpc.

Both on 1 Page

FIGURE I

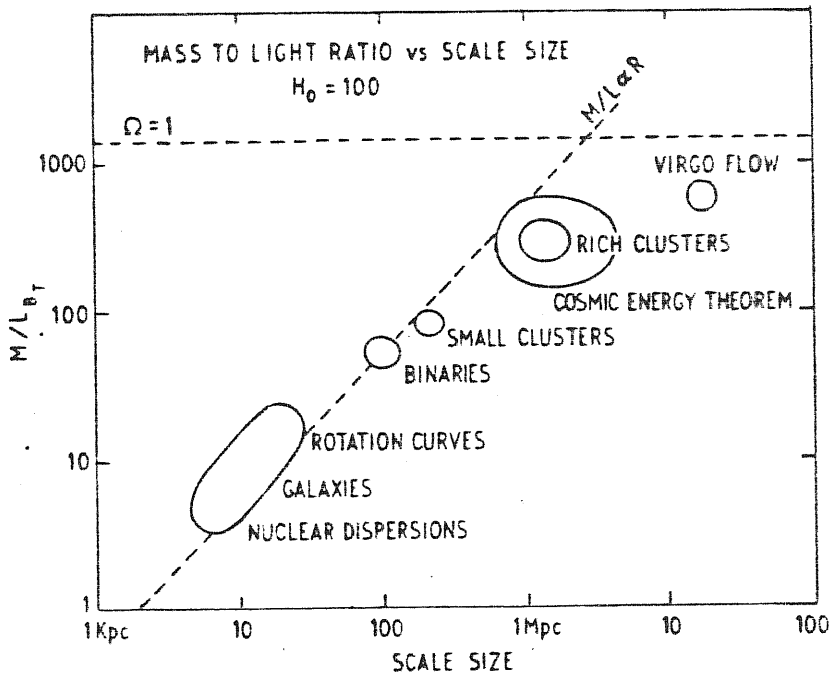

FIGURE 3 Schematic variation of the observed mass to light ratio (in units of $M_\odot/L_\odot$) for objects of increasing scale size; the Hubble constant is taken as 100 Km s^{-1} Mpc^{-1} (Davis *et al.*, 1980).

TABLE I

TABLE II

Typical mass to light ratios (in solar units) versus distance for cosmic structures; compare Figure 3

Region	Distance	M/L
Solar neighbourhood	5–100 pc	1–2
Inner Milky Way	10 Kpc	4–8
Spirals	13 h_0^{-1} Kpc	8–10 h_0
Ellipticals	3 h_0^{-1} Kpc	8–12 h_0
Outer Milky Way	75 Kpc	10–70
Binary galaxies	100 h_0^{-1} Kpc	60–100 h_0
Local group	700 Kpc	80–240
Groups of galaxies	h_0^{-1} Mpc	30–300 h_0
Clustering statistics	1–5 h_0^{-1} Mpc	300–700 h_0
Clusters	h_0^{-1} Mpc	400–600 h_0
Local supercluster	10 h_0^{-1} Mpc	50–110 h_0

If the luminous mass was the only constituent of a galaxy, then we would expect the observed velocities to drop off as $\gamma^{-1/2}$, as implied by eqn.(1.19). But this is not the case in spiral galaxies. The rotational velocities for these galaxies instead remain constant out to large distances, implying that the total mass M interior to γ increases linearly with γ and therefore $\rho \propto \gamma^{-2}$. See figure 2 which gives the observed rotational curves for spiral galaxies(Faber and Gallagher 1979). Measurements on more than 50 spiral galaxies for which rotation curves have been obtained show this effect.(Krumm et.al. 1979;Rubin et.al. 1978)

The dark matter inferred from these rotational curves measurements is found to be atleast 3-10 times the luminous component. Kinematical studies on the globular clusters in our galaxy has shown that the massive halo of our galaxy extends to atleast ~ 40 KPc. (Innanen et.al. 1983). From the orbital dynamics of the Magellanic clouds, it was suggested that the halo of our galaxy must extend to atleast ~ 70 KPc (Lin et.al. 1982). Theoretically, Ostriker and Peebles (1973) found that a massive halo may be required to avoid a bar-like instability and suggested that the disks of spiral galaxies must be imbedded in a stabilizing massive halo. Other evidences supporting massive halos though not as compelling as the galaxy rotation curves, comes from the studies of binary galaxies (Turner 1976 ;Peterson 1979).

Two ways of determining the mass contribution of galaxies to the density, gives an interesting range of uncertainity in the value of Ω . Bright galaxies $[L^* = 1.0 \times 10^{10} h^{-2} L_\odot]$ have a space number density (Kirshner et.al.1979)

$$n_g \sim 0.02 h^3 \text{MPc}^{-3} \qquad (1.20)$$

Taking a typical rotation velocity of a galaxy to be $V \simeq 200 \text{ km s}^{-1}$ at the optical radius, $\gamma \sim 15 h^{-1}$ KPc, we find that the total density due to the luminous parts of galaxies is

$$\Omega_{lum} \sim \frac{n_g V^2 \gamma}{G \rho_c} \sim 0.01 \qquad (1.21)$$

If the observed massive halos are included, this value increases by an order of magnitude. If we extrapolate each galaxy's halo half way to the next galaxy,

FIGURE 2

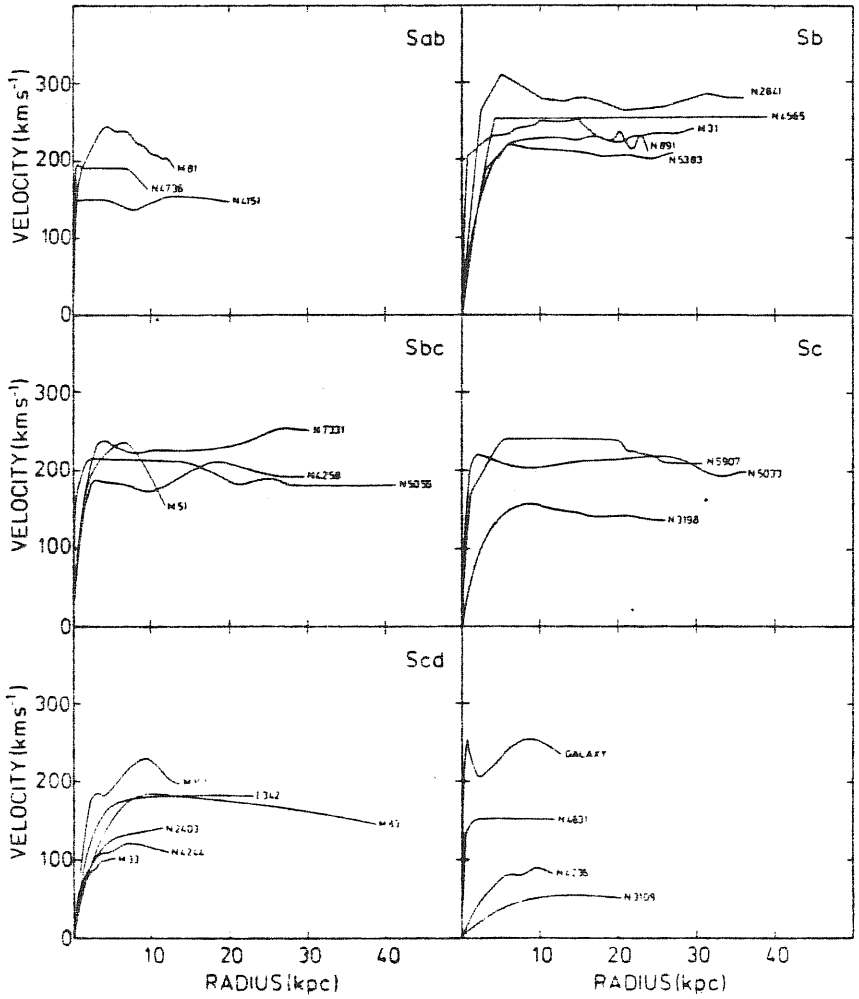

Figure 2 Rotation curves of 25 galaxies of various morphological types from Bosma (1978).

we find (Peebles 1981)

$$\Omega \approx \frac{V^2 n_g^{2/3}}{2G\rho_c} \sim 1 \qquad (1.22)$$

This wide gap of two orders of magnitude between (1.21) and (1.22) can be narrowed by studying the dynamics of systems of galaxies. In fact, strong evidence for the presence of DM comes from the dynamical studies of groups and clusters of galaxies (Faber and Gallagher 1979, Press and Davis 1982 , Davis and Peebles 1983). The problem of DM in clusters first arose when Zwicky in 1933 pointed out that the mass needed to hold the Coma cluster of galaxies together is some orders of magnitude greater than that implied by the estimates of the masses of the galaxies in the cluster obtained from their luminosities. By applying the Virial theorem the masses of these systems can be obtained. Dividing the masses thus obtained by their luminosities, we can find the mass-to-light ratios for these objects.These are similar to the ones given before.

We see from these results that there is a considerable amount of DM in the universe. The nature of this dark matter is still a mystery. We shall see later that various species of elementary particles might provide a natural explanation for this DM.

Multiplying the mass-to-light of the different objects by the luminosity density(eqn.1.17) we obtain the mass density. The typical values are(Faber and Gallagher 1979)

Ω	(Solar neighborhood)	$= 0.004 \pm 0.007\, h_0^{-1}$
Ω	(Galaxies)	$= 0.006 - 0.014$
Ω	(Binary galaxies and groups)	$= 0.04 - 0.13$
Ω	(Clusters)	$= 0.2 - 0.7$

We see that Ω shows a strong correlation with the scale surveyed.The trend is quite clear, suggesting that DM clusters preferentially on larger scales. The value of Ω inferred from these results suggests that though Ω increases with scale there is no evidence that $\Omega = 1$. The largest inferred values of Ω are in the range $0.2-0.6$. Even on the very largest scales observed, that of superclusters with masses $M \sim 10^{15}-10^{16} M_\odot$ the observed Ω never reaches unity.Cosmological models in which the universe passes through a very early de-Sitter " inflationary stage" predict $\Omega = 1$ the Einstein- de Sitter universe(

However, it may be that the amount of DM also increases with scale. That is it may have a distribution that does not fall even on the scales of the giant superclusters. Such a distribution is the only way to reach $\Omega = 1$. Such a distribution would also imply that light emitting matter is not a particularly good tracer of the mass. Another method of estimating Ω is based on the peculiar velocity V_{LG}, of our Local Group (LG) of galaxies toward the Virgo cluster (Davis and Peebles 1983). This method may represent the best near hope of measuring the component of the mass that might be clustered on large scales($\sim 10 h^{-1}$ Mpc). The basic assumption is that the peculiar velocity V_{LG} arises from the gravitational acceleration due to the mass concentrated in the Local Supercluster, the flattened struture containing several thousands of galaxies surrounding the Virgo cluster. As a result of the agreement between V_{LG} measured with respect to a group of distant(~ 50 Mpc) galaxies (Hart and Davies 1982) and the value measured from the dipole anisotropy in the microwave background radiation (Davis and Peebles 1983) we have $V_{LG} \sim 400 \pm 60$ kms^{-1} Assuming that the mass and galaxy number density enhancements represented by the Local Supercluster are the same ($\frac{\delta M}{M} \approx \frac{\delta N}{N} \approx 2$) and neglecting any flattening, we get

$$\Omega = 0.35 \pm 0.15 \qquad (1.24)$$

Though, uncertainities in this value are large. Ω could be larger if the mass density is less concentrated than the galaxy density on supercluster scales or if flattening and the effects of possible under-densities outside the Local Supercluster are accounted for (Hoffman and Salpeter 1982)

Unfortunately for the advocates of $\Omega = 1$ there is no positive and definite evidence for $\Omega = 1$. What is very clear though is that a large amount of matter in the universe is dark.

1.3 THE DARK MATTER

The exact nature of the dark matter is still unknown, but there are arguments that it may not be "baryonic"; That is, it is not made of protons, neutrons and electrons as all ordinary matter familiar to us is. The strongest argument concerning dark matter not being baryonic comes from the big bang nucleosynthesis, which gives us limits on the total amount of baryonic matter present in the universe. This is derived from the combined D and ^{3}He abundances and using the fact that no significant amount of D has been produced since nucleosynthesis.(Yang et.al.1984)

In the early universe, almost all the neutrons which "freeze-out" are synthesised into ^4He. The synthesis process sets in quite suddenly;between $T \sim 10^9 - 3\times10^9$ K the neutron fraction drops dramatically and the deuterium and the tritium abudances peak before dropping slightly as these nuclei are incorporated into helium-4. The abundances are stabilized by $T \sim 0.3 \times 10^9$ K except for the neutron fraction which continues to drop through beta decay. The bulk of the material ends up as ^4He and H. The lack of stable nucleus with atomic no. 5 ensures that only traces of heavier elements like ^7Li are synthesized cosmologically.Virtually all the neutrons end up in giving the helium mass fraction $Y \sim 25\%$. The time evolution of the nuclear reactions is given in figure 3.

The nuclear rates depend on the baryon density at the time of the time of nucleosynthesis and hence, via the expansion of the universe, on the present baryon density. The dependence of the results are shown in the figure 4 (Wagoner 1974 ,1979;Yang et.al. 1984). The following points can be seen from the figure:

(a) The helium abundance is relatively insensitive to the matter density.This is because the helium abundance is determined principally by the neutron-proton ratio at the freezing out temperature which in turn is determined by the cosmological expansion rate at that time. At that epoch, the total density in the universe is dominated by radiation ($\rho_r > \rho_b$) and so the matter density plays secondary role in determining the final abundance of ^4He.

(b) The other light elements D, ^7Li etc. are extremely sensitive to the matter density ρ_b. As ρ_b increases, the destruction cross-sections for D and ^3He into ^4He increase. The D and ^3He abundances decrease while ^4He increases slowly. No significant amount of D has been produced since then. And now,much of the remaining D has been converted into ^4He in stellar burning. The amount of ^3He, on the other hand, has increased in normal stellar processes. The sum of the abundances $D + {}^3He$ today, however, gives an upper limit on $D + {}^3He$ present at nucleosynthesis and this in turn gives a lower limit on the amount of baryonic matter present at the time of nucleosynthesis.

$$\Omega_b h^2 \gtrsim 0.01 \qquad (1.25)$$

The present observed abundances of ^4He, D, ^7Li give an upper limit to the baryonic matter density

$$\Omega_b h^2 \leq 0.034 \qquad (1.26)$$

FIGURE 3

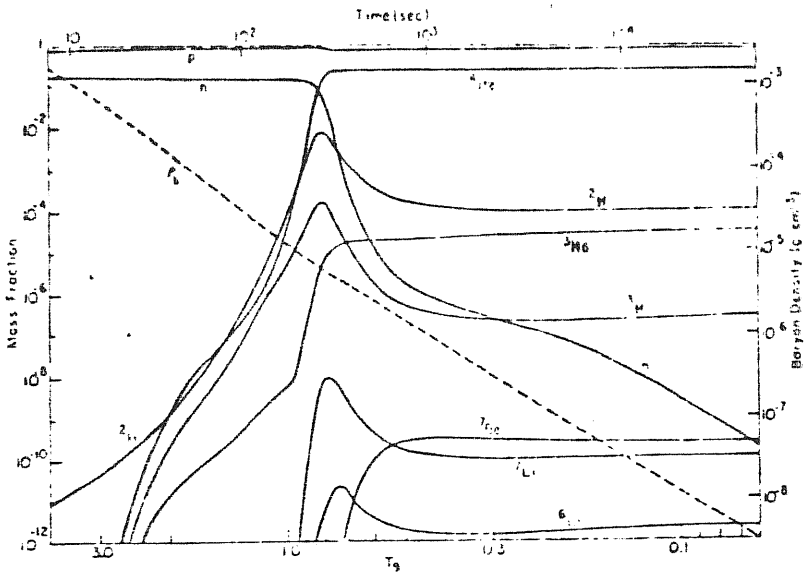

FIGURE 17 Time development of the light element abundances (assuming two massless neutrinos only) (Wagoner, 1974).

FIGURE 4

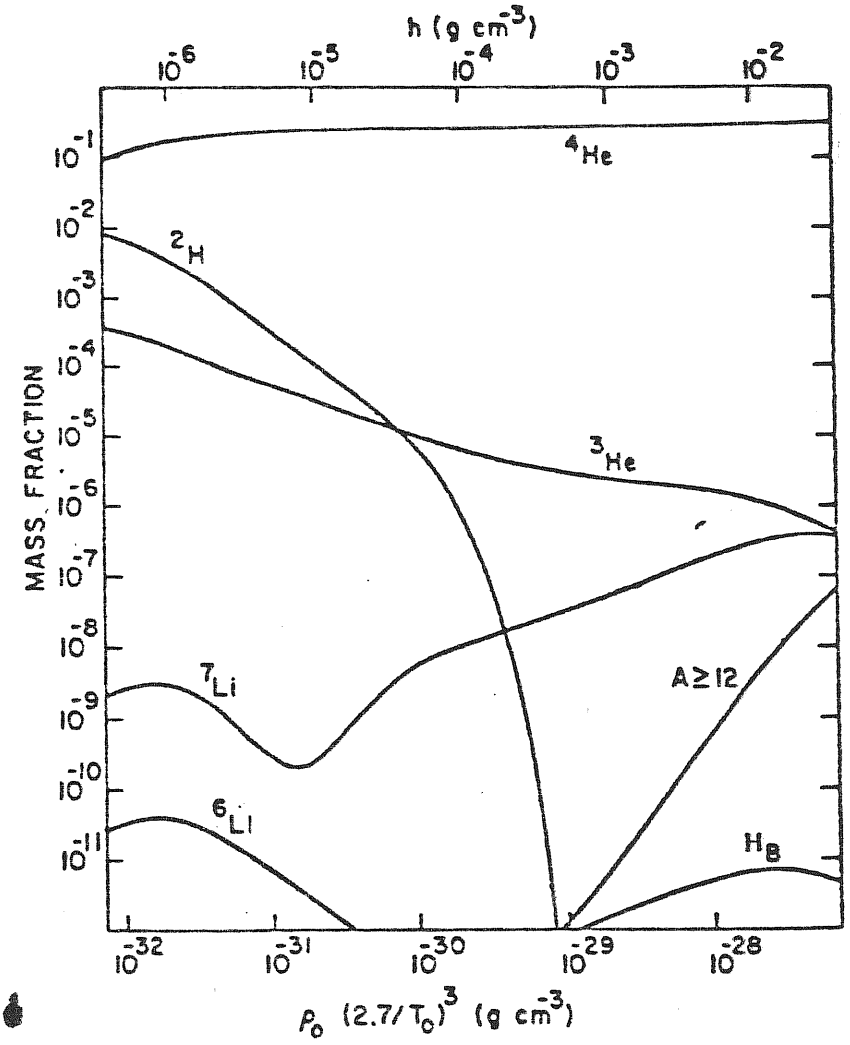

FIGURE 18 Final mass fractions of light elements synthesized in the early universe versus the present baryon density of the universe (for 2 massless neutrinos) (Wagoner, 1974).

Thus, the nucleosynthesis arguments restrict the baryonic matter in the universe to the range

$$0.01 \leq \Omega_b \leq 0.14 \qquad (1.27)$$

We have seen that the mass-to-light ratio keeps increasing on scales larger than binaries and small groups quite drastically and therefore Ω exeeds the upper limit on Ω_b. Therefore we are forced to say that the bulk of matter in the universe in not baryonic. Further, the deviations in the Hubble flow towards the Virgo cluster has given Ω in the range $0.25 \leq \Omega \leq 0.6$ (1.24). The general trend is towards $\Omega \gtrsim 0.15$ and that the dark matter is non-baryonic, though Gott et.al. (1974) suggest that $\Omega \leq 0.1$ and everything is in the baryonic, should not be excluded.

More evidence on the fact that dark matter is not baryonic comes from studies of the massive halos of the spiral galaxies(Hegyi and Olive 1983). The possibilities of the halos being made of baryonic material like gas, snowballs, dust and rocks, "jupiters", low mass stars, dead stars, collapsed objects like the neutron stars and black holes were considered.

Consider a halo made of gas. Since the halo is required to be both stable and static, we have to assume that it is in hydrostatic equilibrium, that is, the halo is maintained only if it is at a temperature T_{eq}. For temperatures less than T_{eq}, the halo would collapse on a gravitational timescale of $\tau_c = \left(3\pi/32 G\rho\right)^{1/2} \sim 5 \times 10^8 yr$, which is much less than the age of the Galaxy. This T_{eq} can be determined from the following argument: from the assumption of the hydrostatic equilibrium

$$\frac{dp_r}{dr} = -\frac{G M_r \rho_r}{r^2} \qquad (1.28)$$

where p_r and ρ_r are the pressure and density respectively, at a radius r and

$$p_r = \left(\frac{2\rho_r}{m_p}\right) KT \qquad (1.29)$$

is the equation of state. Solving the equations (1.28) and(1.29) with $M_r \propto r$ and $\rho \propto r^{-2}$ as the observations indicate, we get

$$T_{eq} = \left(\frac{G m_p}{2k}\right)\left(\frac{M_r}{r}\right) \approx 2 \times 10^6 K \qquad (1.30)$$

for $M_r \approx 10^{12} M_\odot$ at $r \approx 100$ kpc.

A hot gas at temperature T_{eq} however, would emit X-rays, the amount which calculated, exceeds the limits of the observed X-ray background(Silk 1973).

Consider the possibility of the halo consisting of low mass stars or "jupiters" that is, non-nuclear burning objects, with masses $< 0.08 M_\odot$ (Dekel and Shaham 1979). Using a power law distribution function for the number of stars of a given mass, as a function of mass, with the index in the power law matching the observed stellar distribution function, we find that such a halo would radiate more light than is observed.

The possibility of the halo being composed of frozen hydrogen snowballs or dust grains is ruled out because the former would sublimate and the latter would prevent the formation of the observed low-metallicity population-two stars because of their metal elements of atomic number greater than three.

Consider a halo composed of stars with an initial mass greater than $2 M_\odot$, which are now either white dwarfs or neutron stars with minimum masses around $\sim 1.4 M_\odot$. Since stars with masses larger than $2 M_\odot$ must evolve to remnants of only $1.4 M_\odot$, atleast 40 percent of the present halo mass contained in these remnants must have been ejected. The problem is where has the ejected mass gone since it cannot be in the form of hot gas, which would radiate, and it cannot be in the form of cool gas which would quickly collapse into the disk. Further, a significant amount ($\gtrsim 10\%$) of the ejected gas would be in the form of helium and metals(Arnett 1978) and this would contaminate the metal abundances of the oldest stars.

A final possibility is that the halo is composed of black holes. This cannot be possible unless they are extremely efficient in accreting gas or they should be primordial which is a possibility that cannot be ruled out.

Since the nature of the dark matter seems to be non-baryonic and since the conventional possibilities like gas etc. are ruled out, non-conventional possibilities for the form of the dark matter were suggested. Particle physics provided a generous list of weakly-interacting species whose relic abundances can supply the mass density contributed by dark matter. The most popular candidate for the dark matter was the neutrino(Cowsik and McClelland 1972 ; Bond and Szalay 1981). But it was shown that quantum statistics

places an important and an interesting limit on the masses of elementary particles, playing this astrophysical role(Tremaine and Gunn 1979). From the phase space argument it can be shown that the lower limitson the mass of a neutrino, required to be the dark matter are

Dwarf galaxies $m_\nu \gtrsim 250$ eV

Galactic halos $m_\nu \gtrsim 20$ eV

Binaries and Galaxy groups $m_\nu \gtrsim 14\, h_0^{1/2}$ eV

Rich clusters $m_\nu \gtrsim 5\, h_0^{1/2}$ eV

and if globular clusters are dominated by neutrinos, we get the lower limit as

Globular clusters $m_\nu \gtrsim 2$ keV

Inspite of these constraints and the fact that none of the possible candidates for the dark matter have been proved to exist in nature, we find that elementary particles do give a natural explanation for the dark matter. The various candidates suggested and their role in cosmology will be discussed in detail in chapter three.

1.4 THE DISTRIBUTION OF MATTER IN THE UNIVERSE

It has long been suggested that galaxies are not randomly distributed on the sky but often lie in groups and clusters. The clustering of galaxies was first discovered by Herschel in 1811, who did not even know the nature of the nebulae he saw. The clustering of galaxies into groups and clusters is especially striking in plots of the distribution of the nearby galaxies. Figure 5 shows a distribution of galaxies in the northern hemisphere. It appears now that genuinely isolated galaxies are exceptional and perhaps even non-existent.

The distribution of matter is now accepted to be clumpy on all scales ranging from a a simple binary star system to the scales of superclusters, the largest structures known, having masses on the order of 10^{15}–$10^{16}\, M_\odot$(Oort 1983). One approach to study galaxy clustering is to use statistics(Peebles 1980; Fall 1979).

FIGURE 5

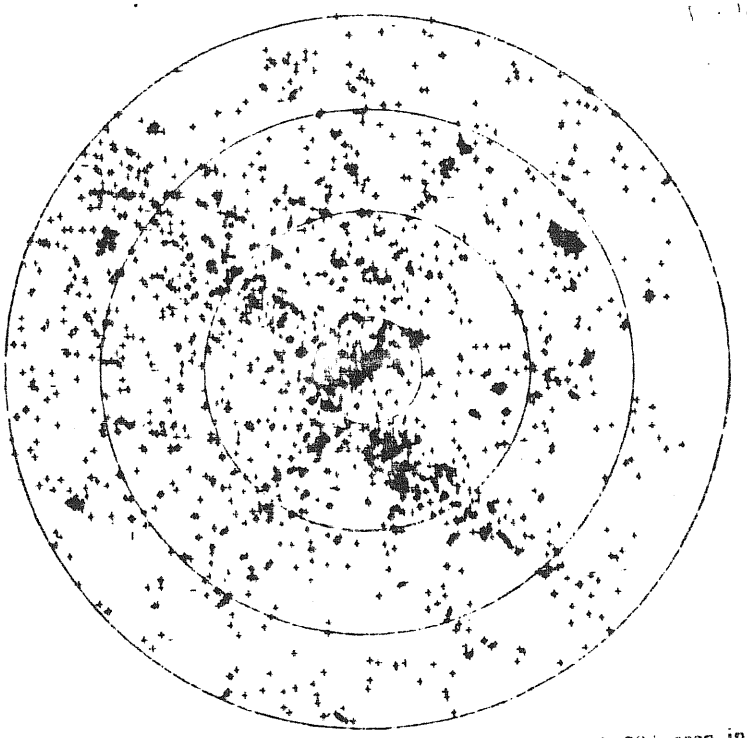

FIGURE 2.5 The distribution of nearby galaxies with $b^{II} > 20°$, seen in projection. The picture shows about 2400 galaxies and is nearly complete to a magnitude limit $B \sim 13$.

The use of statistics has proved to be useful in many ways and the credit for most of the recent work goes to Peebles and his associates at Princeton. They applied the low-order correlation functions to the Zwicky, Lick and the Jagellonian catalogues as a measure of the galaxy clustering. The correlation functions applied to the distribution of galaxies provides important clues about the structure and the evolution of the universe on scales larger than individual galaxies.

THE TWO-POINT CORRELATION FUNCTION

Since the luminous content of the universe exhibits such an overt structure, it is useful to employ some quantitative measure of the clustering. The simplest statistic to use is the two-point correlation function $\xi(r)$. It is defined by the joint probability of finding galaxies centered in the volume elements V_1 and V_2 at a separation r (Peebles 1980):

$$\delta P = n^2 \left[1 + \xi(r) \right] \delta V_1 \delta V_2 \qquad (1.31)$$

where n is the mean space density of galaxies. Consistent with homogeneity and isotropy $\xi(r)$ has been written as a function of separation alone; the galaxy distributions approximate a homogeneous random process. Davis and Geller(1976) found that $\xi(r)$ varies with morphological types in the sense that ellipticals are more strongly clustered than spiral galaxies.

The equation(1.31) tells us that if $\xi(r) > 0$ it implies clustering.
If $\xi = 0$ it implies a purely Poissonian distribution and $\xi < 0$ implies anticlustering, that is, "holes" in the distribution.
Thus, the exact value of $\xi(r)$ provides important facts about the true nature of clustering in the universe.

Peebles(1974) found that the $\xi(r)$ is well approximated by the power-law

$$\xi(r) = \left(\frac{r_0}{r} \right)^{-\gamma} \qquad \left(0.1\ h^{-1}\ \text{MPC} \leq r \leq 10\, h^{-1}\ \text{MPC} \right) \qquad (1.32)$$

$$\text{with} \qquad \gamma = 1.77 \pm 0.04 \ ; \quad r_0 = (4.3 \pm 0.3)\, h^{-1}\ \text{MPC} \qquad (1.33)$$

where r_0 is the normalization quantity.

The normalization quantity comes from Kirshner et.al. (1978) who measured 166 galaxies brighter than an apparent magnitude m=15. The data available to Peebles et.al. consisted of galaxy co-ordinates in projection. Since only a limited amount of information about positions in space is available, most estimates of $\xi(r)$ have been measured through the angular two-point function $w(\theta)$. This angular pair correlation function is given as

$$\delta P(\theta) = \eta^2 [1 + w(\theta)] \, \delta\sigma_1 \, \delta\sigma_2 \qquad (1.34)$$

It is the joint probability of finding two galaxies in the elemental solid angles $\delta\sigma_1$ and $\delta\sigma_2$ separated by an angle θ. η^2 is the mean angular density of galaxies in the sample under consideration. Estimates of w can be made direclty from the counts in a sample for which the positions of individual galaxies on the sky are available.

$\xi(r)$ is related to the $w(\theta)$ through a linear equation which was given by Limber(1954). It takes the form

$$w(\theta) = \left\{ \int_0^\infty dx \, x^4 \phi^2(x) \int_{-\infty}^{+\infty} dy \, \xi[(x^2\theta^2 + y^2)^{1/2}] \right\} \cdot \left\{ \int_0^\infty dx \, x^2 \phi(x) \right\}^{-2} \qquad (1.35)$$

Here $\phi(x)$ is the sample selection function defined as the mean number of sample galaxies per unit volume of space at a distance x from us. The numerical estimates show that the clustering is well-developed. The value of ξ is $\xi(r) \geq 1$ on a scale corresponding to masses below

$$M_* \sim 5 \cdot 10^{14} \, \Omega h^{-1} M_\odot \qquad (1.36)$$

M_* is the characteristic mass scale that separates weak clustering ($M > M_*$) from a well-developed clustering ($M < M_*$) . One of the aims of any theory of galaxy and cluster formation should be an explanation of the magnitude of M_* .

The two-point correlation function is reliably known to be graeter than zero at $r \leq 15 h^{-1}$ Mpc in the Lick sample but is lost in the noise at larger separations. Though structures do extend to larger scales, as density enhancements of galaxies around rich clusters are detected upto $r \sim 40 h^{-1}$ Mpc (Oort 1983), there is no believable evidence on whether $\xi(r)$ is positive or negative at $r \geq 15 h^{-1}$ Mpc.

The statistic $\xi(r)$ gives only a limited description of the clustering and one way to obtain more information is to estimate higher order correlation functions. The three and four-point correlation functions are both well known(Groth and Peebles 1977, Fry and Peebles 1978) . The three-point correlation function has the following form:

$$\zeta(r_{12}, r_{23}, r_{31}) = Q\left[\xi(r_{12})\xi(r_{23}) + \xi(r_{23})\xi(r_{31}) + \xi(r_{31})\xi(r_{12})\right] \tag{1.37}$$

where Q is a constant whose value is 1.29 ± 0.21 (Peebles 1980)
The three-point correlation functions in the Zwicky, Lick, and the Jagellonian samples have been discussed by Peebles and Groth(1975). The eqn.(1.37) is found to be good representation of the data over the scales $0.1 h^{-1}$ Mpc $\leq r \leq 2 h^{-1}$ Mpc .

Fry and Peebles(1978) estimated the four-point correlation function η for the Lick and Zwicky samples. They found that the power-law model gives an adequate description of the estimates for both the catalogues. Results for cross-correlations between galaxies have also been discussed (Peebles 1980).

THE DENSITY FIELD AND $\xi(r)$

It is helpful to think of the distribution of galaxies as representing a fluctuating density field. Also it is convenient to express $\xi(r)$ in terms of the local density of galaxies:

$$\xi_g(r) = \langle \rho(\vec{x})\, \rho(\vec{x}+\vec{r}) \rangle / \langle \rho^2 \rangle - 1$$

$$= \langle \delta\rho(\vec{x})\, \delta\rho(\vec{x}+\vec{r}) \rangle / \langle \rho^2 \rangle \tag{1.38}$$

If the matter in the universe is entirely in the galaxies and their halos, then the observed correlation function (eqn.1.32) should reflect the matter correlation function, that is, $\xi(r) = \xi_g(r)$. Later on we will see how this helps in determining the shape of the primordial fluctuation spectrum that is responsible for the structure we now see in the universe.

The description of galaxy clustering in terms of the correlation functions suggests a gravitational orgin for the structure of matter on scales larger than those of individual galaxies. Clumps with ahigh overdensity should be bound and stable,in which case one can apply the Virial theorem. The mass of a typical ^{clump} is given (Peebles 1976a, 1976b) as:

$$M \sim \bar{\rho}\, \xi(r)^3\, r^3 = \rho\, r_0^{\gamma}\, r^{3-\gamma} \tag{1.39}$$

by using eqn. (1.32)
since

$$v^2 \sim \frac{GM}{r} = G\bar{\rho}\, r_0^{\gamma}\, r^{2-\gamma} \tag{1.40}$$

The one-dimensional mean square velocity $\langle v_{21}^2 \rangle$ between galaxy pairs of separation r_{12} is related to the sum of the accelerations over triplets of galaxies(Peebles 1980 §75)

$$\langle v_{12}^2 \rangle = \frac{6G\bar{\rho}}{\xi(r)} \int_r^{\infty} \frac{dr}{r} \int d^3\vec{z}\, \frac{\vec{r}\cdot\vec{z}}{z^3}\, \xi\left(\vec{r}, \vec{z}, |\vec{r}-\vec{z}|\right) \tag{1.41}$$

if the velocity dispertion is isotropic and clustering is bound and stable. Using eqns.(1.32),(1.37) the equation (1.41) can be written as

$$\langle v_{12}^2 \rangle^{1/2} \approx 800\, Q^{1/2}\, \Omega^{1/2} \left(\frac{r_0}{4h^{-1}}\right)^{\gamma/2} \left(\frac{r}{1h^{-1}\,\mathrm{MPC}}\right)^{0.1} \mathrm{Km\cdot sec^{-1}} \tag{1.42}$$

This relation is called the Cosmic Virial theorem. A measure of the relative peculiar velocities between galaxy pairs provides an estimate of the density parameter Ω ,assuming that the galaxy correlation functions accurately measure the mass distribution.

A CfA redshift survey, carried out by Davis and Peebles(1983) has given

$$\langle v_{21}^2 \rangle \simeq 300 \pm 50\ \mathrm{Km\ sec^{-1}}\ ;\quad r \sim 1\, h^{-1}\ \mathrm{MPC}$$

Using this value and the value of $Q = 1.3$, in the eqn.(1.42) we get

$$\Omega \simeq 0.1 \qquad (1.43)$$

The peculiar velocity studies indicate a low mean matter density in the universe. This result however, does not necessarily exclude a high density universe for it is possible that most of the dark matter is broadly distributed and is not clustered on small scales.

VOIDS AND FILAMENTS

In addition to the largest structures in the universe having high density enhancements, there also regions in the universe completely devoid of any galaxies. These empty regions in space "voids" came up in a redshift survey of galaxies by Kirshner et.al. (1981) who reported of an apparent absence of galaxies in the redshift range $z \approx 0.04 - 0.06$ over a very large area of the sky ($\sim 40^\circ \approx 100\ h^{-1}$ Mpc across), in the direction of Bootes. This zone of depletion corresponds to an enormous volume of the order $\sim 10^6\ h^{-3}\ \mathrm{Mpc}^3$. The density within the holes is 10 % of the mean cosmic density if we are allowed to assume that the number of galaxies is indicative of the local mass density.

Bahcall and Soneira(1982) suggested that the void in Bootes is surrounded by large superclusters , since the void coincides in redshift space with an excess density of clusters and superclusters, specifically Hercules supercluster in the foreground and Corona Borealis supercluster in the background. The observational evidence for smaller volumes of galaxy depletions in the vicinity of superclusters also exists (Chincarini et.al. 1975, Taranghi et.al. 1980, Davis et.al. 1982). These observational results seem to suggest that galaxy voids and large-scale superclusters might be strongly correlated; voids being surrounded by large superclusters.

Besides voids in the universe, on the largest scales matter appears to be in a filamentary structure(Zeldovich et.al. 1982). Although statistical work on these structures is still being developed, preliminary explorations using percolation studies(Shandarin et.al. 1982, Zeldovich et.al. 1982) seem to show that these structures are real. Any theory regarding the formation of galaxies in the universe should take into account the existence of such structures and should account for their presence.

COMPUTER SIMULATIONS

An interesting test of the clustering picture is to simulate on the computer a model galaxy distribution, project this distribution onto the model sky and compare the visual impression of the resulting map with maps of the actual galaxy distribution. This was done using the Lick map as the standard by Soniera and Peebles(1978).

Figure 6 shows the space distribution of the galaxies constructed on this by them. Each fan in the figure represents a slice of the model sky one degree thick and 40° wide. The three fans are placed one above the other at separations of 3.5°. The voids in these figure may be due to statistical fluctuations.

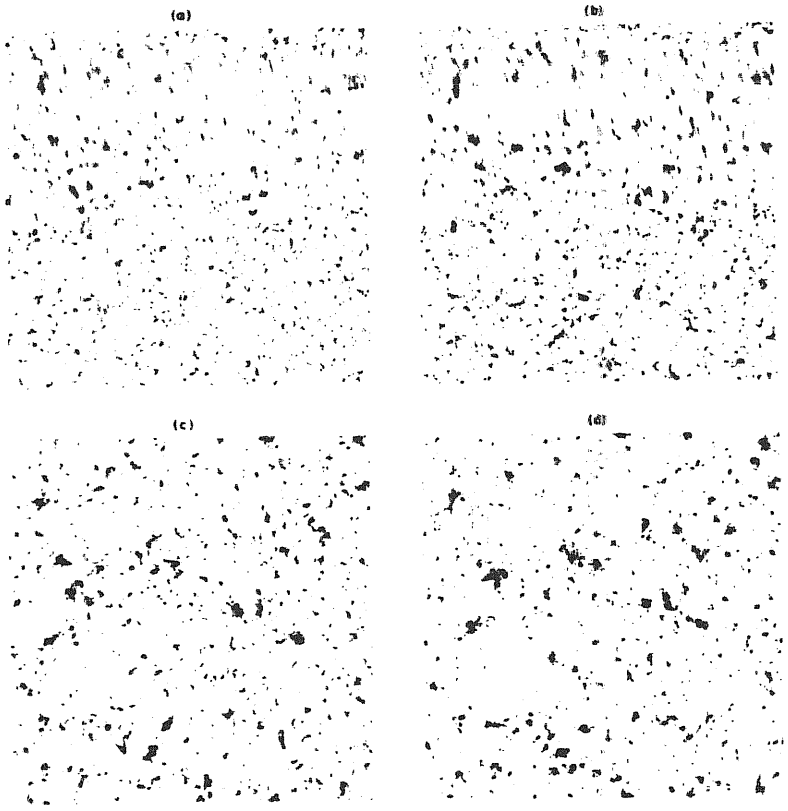

FIGURE 6

FIGURE 5.4 Evolution of clustering in a large N-body simulation ($N = 20{,}000$) with Poisson initial conditions and $\Omega = 1$. (a) Shows positions after the system has expanded by a factor of 5.1; (b) after expansion by a factor of 9.8; (c) after expansion by a factor of 16.0; (d) after expansion by a factor of 28.1.

CHAPTER TWO

THE GROWTH OF STRUCTURE IN THE UNIVERSE

Marring the perfection of the standard model for the universe we see that galaxies exist and are discernibly clustered in aggregrations upto $10^{15} M_\odot$ or more and on scales ranging upto $30\ h^{-1}$ MPC corresponding to $\approx 1\%$ of the present day horizon size. The existence of such structure implies that the early universe must have contained some irregularities in the density of matter, because making of galaxies requires some sort of fluctuation which can evolve under its self-gravity. Now it is generally accepted that the universe was close to Friedmannian at early times but that small irregularities existed which grew by the mechanism of gravitational instability forming the present structure we now observe in the universe.

2.1 GRAVITATIONAL INSTABILITY

The fundamental cause for structure in the universe is the mechanism of gravitational instability. The idea that galaxies have grown as a result of gravitational instability can be traced to Jeans in 1902. The early universe was nearly uniform in density but not perfectly so and many regions were overdense enough to gravitationally bound. These bound lumps expanded for a while, reached maximum radii and then recollapsed, settling quickly into dynamical equilibrium. Depending on the original mass of the bound lump, it may be today be identified with a galaxy($10^6 - 10^{12} M_\odot$),a group or clusters of galaxies($10^{13} - 10^{15} M_\odot$) or a supercluster($10^{15} - 10^{16} M_\odot$).

The evolution of a density inhomogeneity as function of time can be understood by comparing its size with three characteristic scales: (a) the horizon scale, (b) the Jeans mass, (c) the damping scale

(a) The horizon scale

The spatial distance to the horizon at a time t is given by $\lambda_H = ct$ associated with it is a characteristic mass

$$M_H = \frac{4}{3} \pi \rho_m [ct]^3 \qquad (2.1)$$

where ρ_m is the baryon density. The eqn.(2.1) gives the mass of baryons within the horizon at a time t .

In a radiation-dominated universe (RD) the scale factor $R \sim t^{1/2} \sim (1+z)^{-1}$
Correspondingly, the mass within the horizon is $M_H \sim (1+z)^{-3}$
For $z < z_{eq}$ a matter-dominated universe, $R \propto t^{2/3}$ and $M_H \sim (1+z)^{-3/2}$
So, we get for M_H :

$$M_H \simeq 10^{16}\, \Omega h^2 \left(\frac{1+z_{eq}}{1+z}\right)^3 M_\odot \quad \text{—— RD} \qquad (2.2)$$

$$M_H \simeq 2 \times 10^{17} (\Omega h^2)^{-1/2} \left(\frac{1+z_{rec}}{1+z}\right)^{3/2} M_\odot \quad \text{—— MD} \qquad (2.3)$$

(b) The Jeans mass

The Jeans length scale λ_J , is of fundamental importance in the gravitational instability picture. This is the minimum scale on which pressure gradients in a sphere can balance the gravitational forces. For scales $\lambda > \lambda_J$, gravity dominates the dynamical motions, whereas for $\lambda < \lambda_J$ pressure dominates and the inhomogeneity behaves like an acoustic wave.
In an expanding universe with $\Lambda = 0$, the characteristic time for collapse or expansion is

$$t \sim (G\rho)^{-1/2} \qquad (2.4)$$

where ρ is the density of the medium.
If the velocity of sound in the matter(assuming it behaves like a perfect fluid) is c_s the Jeans lenght is given by

$$\lambda_J = \left(\frac{\pi c_s^2}{G\rho}\right)^{1/2} \qquad (2.5)$$

Since $c_s < c$, this is always less than the scale of the horizon. The corresponding Jeans mass is

$$M_J = \frac{4\pi}{3} \rho \left(\frac{\lambda_J}{2}\right)^3 \qquad (2.6)$$

All density fluctuations larger than the Jeans mass tend to grow due to gravity, while perturbations below the Jeans mass M_J, oscillate with constant amplitude, as ordinary sound waves. Thus the Jeans mass M_J, is the characteristic mass which divides a growing mode from a stationary mode.

Prior to recombination, the matter and radiation are closely coupled, and they can be regarded as a single composite fluid where the pressure is mainly due to photons, that is, $P = P_\gamma \simeq \frac{1}{3}\rho_\gamma c^2$. The sound speed in this medium is given by(Rees 1971)

$$c_s^2 = \left(\frac{\delta P}{\delta \rho}\right)_{adiabatic} \quad \text{where}$$

$$\delta\rho = (3\rho_m + 4\rho_\gamma)\frac{\delta T}{T}$$

$$\delta P = \frac{4}{3}\rho_\gamma \cdot \frac{\delta T}{T} \qquad (2.7)$$

Here ρ_m and ρ_γ are the densities of matter and radiation field respectively. Thus

$$c_s^2 = \frac{c^2}{3}\left[\frac{1}{1+\frac{3}{4}\frac{\rho_m}{\rho_\gamma}}\right] \qquad (2.8)$$

Since it is the radiation-dominated era, $\rho_\gamma \gg \rho_m$ and so we get $c_s \simeq \frac{1}{\sqrt{3}}c$.

Since c_s is only slightly smaller than the c, the corresponding Jeans length is only slightly smaller than the horizon scale. So $M_J \sim M_H$

Therefore for $z \gtrsim z_{rec}$, we have the Jeans mass as

$$M_J \simeq 10^{17}\left[\frac{1+z_{eq}}{1+z}\right]^3 \frac{(\Omega h^2)^\alpha}{\left[1+\left(\frac{1+z_{eq}}{1+z}\right)^3\right]} \qquad (2.9)$$

where $\alpha = 1$ for RD ; $\alpha = -2$ MD

radiation

After, recombination, when matter and have decoupled ,the relavent sound speed for the matter is only

$$c_s^2 = \left(\frac{5}{3}\ \frac{kT}{m_p}\right) \tag{2.10}$$

The Jeans mass, correspondingly drops to

$$M_J \simeq 10^6 (\Omega h^2)^{-1/2} \left(\frac{1+z}{1+z_{rec}}\right)^{3/2} M_\odot \tag{2.11}$$

On scales larger than this, density fluctuations in the linear regime can grow until the present epoch.

(c) The damping scale

Though perturbations on scales $\lambda \ll \lambda_J$ behave as acoustic modes, it is not possible to propagate disturbances of arbitrarily small wavelength through the universe.Limitations on the wavelength are imposed by viscosity and thermal conductivity of the cosmic fluid,since both these processes can remove energy from sound waves of sufficiently high frequency. If the damping time scale is shorter than the cosmic expansion time scale, the wave will be efficiently damped before the universe has had time to expand by an appreciable factor.

In the pre-recombination era,both viscosity and thermal conductivity are governed by the Thomson scattering process. The mean-free-path of a photon with respect to electron scattering is

$$\lambda_{es} = \frac{1}{n_e \sigma_T} \simeq 10^{24}\ n_e^{-1}\ cm \tag{2.13}$$

where σ_T is the Thomson cross-section and n_e is the free electron density. Associated with this is a characteristic mass

$$M_{\tau=1} = \lambda_{es}^3\ n_e\ m_p \simeq 10^{48}\ n_e^{-2}\ gm \tag{2.14}$$

For $z > z_{rec}$

$$M_{\tau=1} \simeq 10^6 (\Omega h^2)^{-2} \left(\frac{1+z_{rec}}{1+z}\right)^6 M_\odot \tag{2.15}$$

Another relevant damping scale is the Silk's mass. Adiabatic density fluctuations on sufficiently small scales are damped by both the action of viscosity and radiation diffusion. The former process acts to smooth out velocity gradients, while the latter smooths out temperature gradients. The damping of these fluctuations was first calculated independently by Michie(1967), Peebles(1967) and Silk(1968), though only the latter work was published. Hence the associated damping mass is called the Silk mass today.

For $z_{eq} > z > z_{rec}$, the Silk damping mass is

$$M_{D.Silk} = \left(M_{\Omega=1} \, M_H(MD) \right)^{1/2} \propto 5 \times 10^{12} (\Omega h^2)^{-5/4} \left(\frac{1 + z_{rec}}{1 + z} \right)^{15/4} M_\odot \qquad (2.16)$$

At the on set of recombination , perturbations on scales smaller than equation (2.16) are attenuated.

2.2 THE DENSITY PERTURBATIONS

Galaxies belie the homogeneity of the universe not just today but all the way back to t=0, since no means of growing the inhomogeneities spontaneously from the standard model has yet been found. The problem of galaxy formation is to postulate some natural set of perturbations at t=0 and then propagate these perturbations through a few times 10^9 years atleast and then demonstrate that they give rise to galaxies, clustering of galaxies voids, filaments etc. , consistent with the present observations(Peebles 1980, Rees 1978, Gott 1977).

The origin of the density fluctuations required to produce galaxies is still an unsolved problem. Ideally, one would like to be able to show that the flutuations could arise naturally, spontaneously and then grow to have the value we require. Unfortunately, it has proved very difficult to explain how the required fluctuations could arise spontaneously and most cosmologists have concluded that fluctuations just have to be into the initial conditions of the universe at, say, an epoch as early as the Planck time. This is not a satisfactory attitude since ultimately, one has more or less given up the hope of explaining the origin of galaxies!

Many pictures in which fluctuations could have arisen spontaneously have been suggested but none of them is conclusive yet. One of the scenarios is where the fluctuations are induced by quantumgravity effects at the Planck time(Wheeler 1957, Harrison 1970). Another scenario was suggested where the fluctuations could have arose from false vac uum effects at the grand unification epoch(Hawking 1983, Guth 1982, Bardeen et.al. 1982)

The fluctuations could have arisen in an initially homogeneous universe through statistical effects if the universe forms "grains" at some phase transition. At some level the universe is bound to develop graininess as we know that matter is in discrete particles like protons at some later epoch. However, grains of only 10^{-24} gms. are far too small to produce galaxies . If graininess developes on much larger scales, say when the universe undergoes a phase transition , then it might be possible to have large fluctuations. Unfortunately, such fluctuations were found not large to produce galaxies, unless the grains formed at an implausibly late epoch(Carr and Silk 1983).

In the standard model, large scale structure forms when perturbations in density $\delta \equiv \frac{\delta\rho}{\rho}$ grow to $\delta \geq 1$, after which they cease to expand with the Hubble flow. The evolution of the perturbations is generally discussed separately at the two epochs $t < t_{rec}$ and $t > t_{rec}$. Two specific Fridmann models are considered ;The Einstein-de Sitter model ($\Omega = 1$) and the "open" model($\Omega = 0.1$).

For the $\Omega = 1$ model, the mass within the horizon at ($M_J \sim M_H$) is $\sim 10^{17} M_\odot$. Fluctuations on the mass scales of galaxies and clusters of galaxies thus come within the horizon during the radiation-dominated era and are frozen at approximately their initial amplitudes $\frac{\delta\rho}{\rho}$ until recombination because the radiation and matter are locked together by Thomson drag, and the radiation fluid is quite stiff.Here since the sound speed is nearly the speed of light, $c_s = \frac{1}{\sqrt{3}} c$ .At recombination, the Jeans mass drops to $\sim 10^5 M_\odot$ and on all scales larger than this, density fluctuations in the linear regime grow according to

$$\frac{\delta\rho}{\rho} \propto (1+z)^{-1} \propto t^{2/3} \qquad (2.17)$$

from recombination until the present epoch(Rees 1971). Thus,for galactic mass scales $10^{11} - 10^{12} M_\odot$, growth by a factor of 1000 is possible for perturbations in the linear regime between recombination and the present epoch. Once a perturbation has grown to the point where $\frac{\delta\rho}{\rho} \sim 1$, non-linear effects accelerate the enhancement process. However, density fluctuations at recombination greater than $0.1\ \%$ are needed to produce galaxies by the present epoch in an $\Omega = 1$ model. When the universe is matter-dominated, the $M_J \sim 10^{17}$ (eqn.2.9). Fluctuations on mass scales larger than M_J can grow until the present $\left(\frac{\delta\rho}{\rho}\right) \propto R$. But fluctuations on mass scales slightly less than the mass $10^{17} M_\odot$ remain at the amplitude at which they entered the horizon until the epoch of recombination(Gott and Rees 1975).

In the $\Omega = 0.1$ model the growth of perturbations does not start until the epoch corresponding to a redshift $1+z \simeq 10^4 \Omega h^2$

because of Thomson drag and because small matter fluctuations do not grow in a universe dynamically dominated by radiation(Meszaros 1974). In general, perturbations in the matter do not grow prior to $(1+z_{eq})$ even if this is later than recombination. For the $\Omega = 0.1$ universe we have $R \propto t^{1/2}$ during radiation-dominated, $R \propto t^{2/3}$ for matter-dominated and $R \propto t$ from $(1+z_{open}) = \Omega^{-1} = 10$ up through the present epoch. The last phase is that in which the density has dropped significantly below the critical value ρ_c, so that matter no longer significantly decelerates the Hubble expansion, and a linear expansion prevails. At recombination $M_J \sim 10^6 M_\odot$, so perturbations larger than this are free to grow according to eqn(2.17), but for z=10 until the present epoch, we have

$$\frac{\delta\rho}{\rho} \sim \text{Constant} \qquad (2.18)$$

for perturbations in the linear regime. Thus in the $\Omega = 0.1$ model, growth by a factor of 100 is possible in the linear regime, requiring perturbations $\geq 1\%$ at recombination.

For the gravitational instability picture to work, we need $\Omega > 0.01$ because at this limiting value we have $(1+z_{eq}) = (1+z_{open}) = \Omega^{-1} = 10^2$. Perturbations cannot grow prior to $(1+z_{eq})$ because the universe is radiation-dominated, and cannot grow subsequent to this because the universe is so open that it has already entered its linear expansion phase. We see that this provides a rough lower bound on the density parameter Ω_b.

2.3 THE FLUCTUATION SPECTRUM

Since the matter distribution in the universe is clumpy not just on the scale of galaxies, but on all scales upto 100 MPc, it is therefore important and useful to view galactic fluctuations in the context of a general spectrum of fluctuations which extend to much larger scales. A clue to the orgin of fluctuations may be contained in the form of this spectrum.

Zeldovich(1972) has suggested that the proper place to discuss density fluctuations is when they first come within the horizon. Density fluctuations on the scale of the horizon tell how different parts of the universe are sewn together prior to their coming in causal contact. It is commonly assumed that the amplitude of a fluctuation when it first comes within the horizon varies as some power of the mass contained within the horizon at that time:

$$\left(\frac{\delta\rho}{\rho}\right)_H = \varepsilon \left(\frac{M_H}{M_*}\right)^{-\alpha} \qquad (2.19)$$

where the power-law index α and the amplitude(fixed by M_*) as free parameters.

Zeldovich suggested that this spectrum should have the simplest shape. In particular, it should have no preferred mass scales. This is often referred to as constant curvature fluctuations. Zeldovich suggested a spectrum with $\alpha = 0$ and

$$\left(\frac{\delta\rho}{\rho}\right)_H = K \tag{2.20}$$

where K is some constant. Zeldovich argues that the constant K might be related to the total entropy per baryon, the entropy being generated by the damping of short wavelength perturbations. He suggests $K \sim 10^{-4}$. This is the simplest possible primordial density fluctuation spectrum. If we choose the $\alpha < 0$, the universe becomes more and more clumpy with time. Eventually $\left(\frac{\delta\rho}{\rho}\right)_H \sim 1$ and the universe becomes non-Friedmannian. Since the universe is so uniform today as the cosmic background near isotropy suggests, it is hard to accept $\alpha < 0$. On the other hand, if we choose $\alpha > 0$, it implies that the universe was very non-Friedmannian at early times. Here it is likely that order-unity fluctuations on scales of the horizon would lead to a profilic production of black holes with masses $\simeq M_*$ (Carr 1975, Barrow and Carr, 1978) and would disrupt the standard picture of nucleosynthesis. This is unattractive, but to avoid these problems, some physical process is required which cuts off the spectrum(2.19) such that $\frac{\delta\rho}{\rho} << 1$ for $M \lesssim M_*$ (Press and Vishniac 1980).

We have seen that the two-point correlation function $\xi(r)$ is well approximated by a power law and the spatial correlation function for matter is

$$\xi_\rho(|r|) = \langle \rho(\vec{x})\rho(\vec{x}+\vec{r})\rangle / \langle\rho\rangle^2 - 1$$

$$= \langle \delta\rho(\vec{x})\delta\rho(\vec{x}+\vec{r})\rangle / \langle\rho\rangle^2$$

Since $\xi(r)$ approximates a power law, we would suppose that the spectrum of the initial perturbations is a power law (Peebles 1974)

$$|\delta_k|^2 \propto k^n \tag{2.21}$$

where δ_k is the Fourier tranform of $\left[\rho(x)/\langle\rho\rangle - 1\right]$

δ_k has randomly assigned phases. Then for fluctuations with diameter $\sim k^{-1}$ have an amplitude

$$\left(\frac{\delta\rho}{\rho}\right) \propto M^{-1/2-n/6} \qquad (2.22)$$

n is related to the spectral index α as $n = 6\alpha + 1$

2.4 THE TYPES OF FLUCTUATIONS

There are two generic types of perturbations, which by the process of gravitational instability might evolve into galaxies etc. (Peebles 1980). The two types are (a) adiabatic perturbations and (b) isothermal perturbations.

(a) Adiabatic perturbations

These involve perturbations in both matter and radiation components of the universe during the radiation era, so

$$\frac{\delta\rho_\gamma}{\rho_\gamma} \neq 0 \neq \frac{\delta\rho_B}{\rho_B}$$

Here the entropy per baryon remains constant; $\frac{\delta S}{S} = 0$

(b) Isothermal perturbations

These arise from perturbations of the baryon density, while the radiation remains smooth

$$\frac{\delta\rho_\gamma}{\rho_\gamma} = 0 \quad , \quad \frac{\delta\rho_B}{\rho_B} \neq 0$$

Here the entropy per baryon is not conserved , $\frac{\delta S}{S} \neq 0$. Therefore, these are also called the "entropy perturbations".

The characteristic spectrum of inhomogeneities surving the radiation era of the universe differs according to whether the initial perturbation is isothermal or adiabatic. In both cases, there exists a characteristic mass below which irregularities are damped out by pressure.

For the adiabatic perturbation, photon diffusion has time to erase inhomogeneities during the radiation era that are smaller than (Silk 1981)

$$M_D^{ad} \sim \frac{1.2 \times 10^2 \, \Omega^{-2} h_0^{\,4}}{(1 + 0.04 \, \Omega^{-1} h_0^{-2})^3} \, M_\odot \qquad (2.23)$$

For $\Omega = 1$, $M_D^{ad} \sim 10^{12} M_\odot$; for $\Omega = 0.1$, $M_D^{ad} \sim 10^{15} M_\odot$

In the case of isothermal perturbations the damping scale M_D^{is}, is condiderably smaller and is just the Jeans mass determined by the baryon pressure. This is of the order

$$M_D^{is} \sim 10^5 \, (\Omega h^2)^{-1/2} \, M_\odot \qquad (2.24)$$

The fate of adiabatic perturbations obeying $n = 1$,spectrum(commonly referred to as the Harrison-Zeldovich spectrum, Harrison 1970, Zeldovich 1972) has been studied by Doroshevich et.al. (1974). At recombination, one finds no significant fluctuations on scales smaller than M_D^{ad} ,but on allscales larger than M_d^{ad} fluctuations are of the order of K . These sound waves involve peculiar velocities $\delta v \sim c\left(\frac{\delta\rho}{\rho}\right) \sim K$ At recombination, the restoring force due to radiation suddenly disappears; regions that happened to be contracting will contract by an amount $\delta v \, t_{rec}$ where t_{rec} is the Hubble expansion time at recombination. The velocity perturbations thus lead to baryon density fluctuations

$$\left(\frac{\delta\rho}{\rho}\right)_{baryon} \sim -3\left(\frac{\delta r}{r}\right) \sim \frac{3\,\delta v \, t_{rec}}{r} \propto r^{-1}$$

Since $M \propto r^3$ this leads to a baryon density fluctuation spectrum

$$\left(\frac{\delta\rho}{\rho}\right)_{baryon} \propto M^{-1/3} \qquad (2.24)$$

The equation (2.24) relies on velocity overshooting to build baryon perturbations larger than the original adiabatic perturbations. This leads to a maximum amplification of ~ 50 at scales just above M_0^{ad} . Press and Vishniac (1980) demonstrated that this overshooting concept is not correct and showed by detailed photon-transport

computations that the amplification factor is only ~ 2 . This poses difficulties in the model picture given by Doroshkevich et.al. They favor adiabatic perturbations in a $\Omega = 0.1$ model of the universe. Their density fluctuation leads to formation of protoclusters of galaxies of mass $10^{14} M_\odot$. Upon collapse of such a protocluster, shock waves would form giving rise to dense flat regions of matter, the "pancakes" that could fragment into galaxies via the usual Jeans instability. Production of bound protoclusters of masses $10^{14} M_\odot$ requires $\delta\rho/\rho \sim 10^{-2}$ and therefore $K \sim 2.2 \times 10^{-4}$. However, Sunyaev and Zeldovich(1972) have shown that collapse to a pancake in one direction may occur while a protocluster is expanding in the other two directions, so protoclusters can be slightly unbound and $K = 10^{-4}$ is acceptable. If the adiabatic scheme is applied to $\Omega = 1$ universe then such problems would not arise. However this requires the post-recombination overshooting discussed before. Without this the value of K must be much higher to produce galaxies: $K > 5 \times 10^{-3}$ for $\Omega = 0.1$ and $K > 10^{-3}$ for $\Omega = 1$. But this produces fluctuations in the microwave background of the order $(\delta T/T) > 10^{-3}$ which exceeds the present observational limits. This is a serious draw back for the adiabatic perturbations. Press and Vishniac (1980) suggested that this problem can be solved if $n = 4$ instead of Zeldovich's spectrum, for this spectrum is steep enough so that the large scale microwave background isotropy is not violated. But the $n = 4$ spectrum runs into trouble at the other end of the spectrum, because it predicts order-unity fluctuations at $10^8 M_\odot$ and below. Press & Vishniac themselves pointed out that this would seriously disturb the primordial nucleosynthesis argument.

The fate of isothermal fluctuations obeying the Zeldovich spectrum $n = 1$, has been studied by Gott and Rees(1975). We have here $\left(\frac{\delta\rho}{\rho}\right)_{total} \sim 10^{-4}$ on the scale of horizon at all times. Now for isothermal perturbations

$$\left(\frac{\delta\rho}{\rho}\right)_{total} = \left(\frac{\delta\rho}{\rho}\right)_{baryon} \cdot \frac{\rho_{baryon}}{\rho_{total}}$$

Since the universe is radiation-dominated for epochs of interest $\rho_{total} \propto R^{-4}$, $\rho_{baryon} \propto R^{-3}$ so $\frac{\rho_{baryon}}{\rho_{total}} \propto R$. Since $M_H \propto t$, $R \propto t^{1/2}$, so $M_{H,total} \propto R^2$ and $M_{H,bary} \propto R^3$ Expressing the density fluctuations in terms of the mass scale in baryons we have

$$\left(\frac{\delta\rho}{\rho}\right)_{baryons} \propto M^{-1/3}$$

These baryon flutuations are not subject to damping and cannot grow because they are locked to the radiation via Thomson scattering, so they remain at this amplitude until recombination. For $K = 10^{-4}$, $\left(\frac{\delta\rho}{\rho}\right)_{baryon} \sim 1$ at scales of $10^5 M_\odot$ ($\Omega = 1$) or $10^7 M_\odot$ ($\Omega = 0.1$). Since the density of baryons never be negative, at smaller scales equal positive and negative total-density fluctuations of amplitude $K = 10^{-4}$ cannot be produced by baryon fluctuations alone.

The value of k can be estimated by matching the observed amplitude of the covariance function. Gott and Rees(1975) find $k \sim 1.5 \times 10^{-4}$ and 2.2×10^{-4} for $\Omega = 1$ and $\Omega = 0.1$ models respectively. This predicts fluctuations in microwave background $\delta T/T \sim k \sim 10^{-4}$ on angular scales greater than 2° for $\Omega = 1$ and greater than 6° for $\Omega = 0.1$, provided the last scattering surface is at $\sim 10^3$. This is compatible with the the observational limits on the microwave background. The isothermal picture is consistent with the observations but till now we have no detailed mechanism to produce the perturbations.
In addition to these fundamental types of primordial perturbations, it has been noted that subsequent hydrodynamic effects(detonation waves) can make small seed perturbations grow(Ostriker and Cowie 1980). Thus if initial seeds can be formed via either adiabatic or isothermal modes, then if they explode and their explosions stimulates other explosions, then large amounts of matter can be moved about even on scales larger than the initial seed perturbations. Such a situation might arise if the quark-hadron transition produced planetary mass black holes which clustered baryons about and subsequently exploded(Freece et.al. 1983).

2.5 GALAXY FORMATION

The minimum size of the surviving inhomogeneities in the adiabatic and isothermal cases suggests two different process of galaxy formation.In the case of pure adiabatic perturbations, the first objects to condense out of the expanding universe are masses of the order of galaxy clusters.Here, large scale perturbations on a scale greater than the damping mass M_D^{ad} must reach the nonlinear stage of growth before galaxies can form. During this growth, initally small anisotropies in the perturbation spectrum are strongly amplified into highly flattened structures, or the "pancakes". If the matter infalling during pancake formation is pressure-free, then as it accumulates in the midplane of the pancake a caustic surface eventually forms at this midplane where streamlines intersect, making the density momentarily infinite there. For a collisional fluid(like the baryon-electron component of the universe), shock waves must develop in the midplane, rather than a caustic (actually one shock on either side of the midplane), which dissipate the kinetic energy of infall by heating the gas, enabling it to cool radiatively in the post-shock flow to a temperature $\leq 10^9 K$. The high density and low temperature of this thin, central sheet ultimately results in its fragmentation and, eventually, in galaxy formation.

Since the density anisotropies are assumed to be small, linear theory of perturbation may be used to discuss the early phases of the picture. Zeldovich(1970) developed the following approximation to treat the growth of adiabatic perturbations.

It actually remains a good approximation even a little beyond the linear regime. The position of a particle $\vec{r}$ is approximated as function of its comoving Lagrangian position $\vec{q}$ and of time t by

$$\vec{r} = a(t)\vec{q} + b(t)\vec{p}(\vec{q}) \qquad (2.25)$$

The first term gives the unperturbed background and the second term $b(t)\vec{p}(\vec{q})$ represents the initial irregularity in the matter distribution, which is assumed to be small. The density in the vicinity of each particle at a later time t, is given by

$$\rho(t) = \frac{\bar{\rho}(t)}{|\partial\vec{r}/\partial q|} = \frac{\bar{\rho}(t)}{|\delta_{ij} + b(t)\partial p_i/\partial q_j|} \qquad (2.26)$$

where $\bar{\rho}(t)$ is the mean density in the universe.
By extrapolating the result of equation (2.26), infinite density is achieved at some time t when the determinant inthe equation vanishes. Thus, the matter will pile up into sheets(pancakes) along the surfaces defined by the condition

$$\left|\frac{\partial\vec{r}}{\partial\vec{q}}\right| = 0$$

Figure 7 shows a 3-Dimensional N-body simulation(Davis et.al. 1983) where the Zeldovich approximation theory is compared with the computer results. From the figure we see that the Zeldovich approximation compares very well with the N-body simulation, especially at early times. At late times Zeldovich's approx. fails to reproduce some of the features seen in the N-body simulation- the filamentary structures. Two-dimensional studies have been done by others(Melott 1983,Doroshkevich et. al. 1980) and the results are compatible with Zeldovich's theory.
Since in this theory galaxy formation proceeds by the fragmentation of "pancakes" this theory is known as the "pancake scenario". Also, since large- structures are formed first, and galaxies later, this is popularly called the "top-down" picture.

However the pancake scenario runs into serious trouble by conflicting with the microwave background temperature fluctuations observed. The residual irregularities in the microwave background offer an extremly important test for the theories of galaxy formation. The present anisotropy in the microwave background(MBR) is correlated with the density variations at recombination for the adiabatic case, because the

FIGURE 7

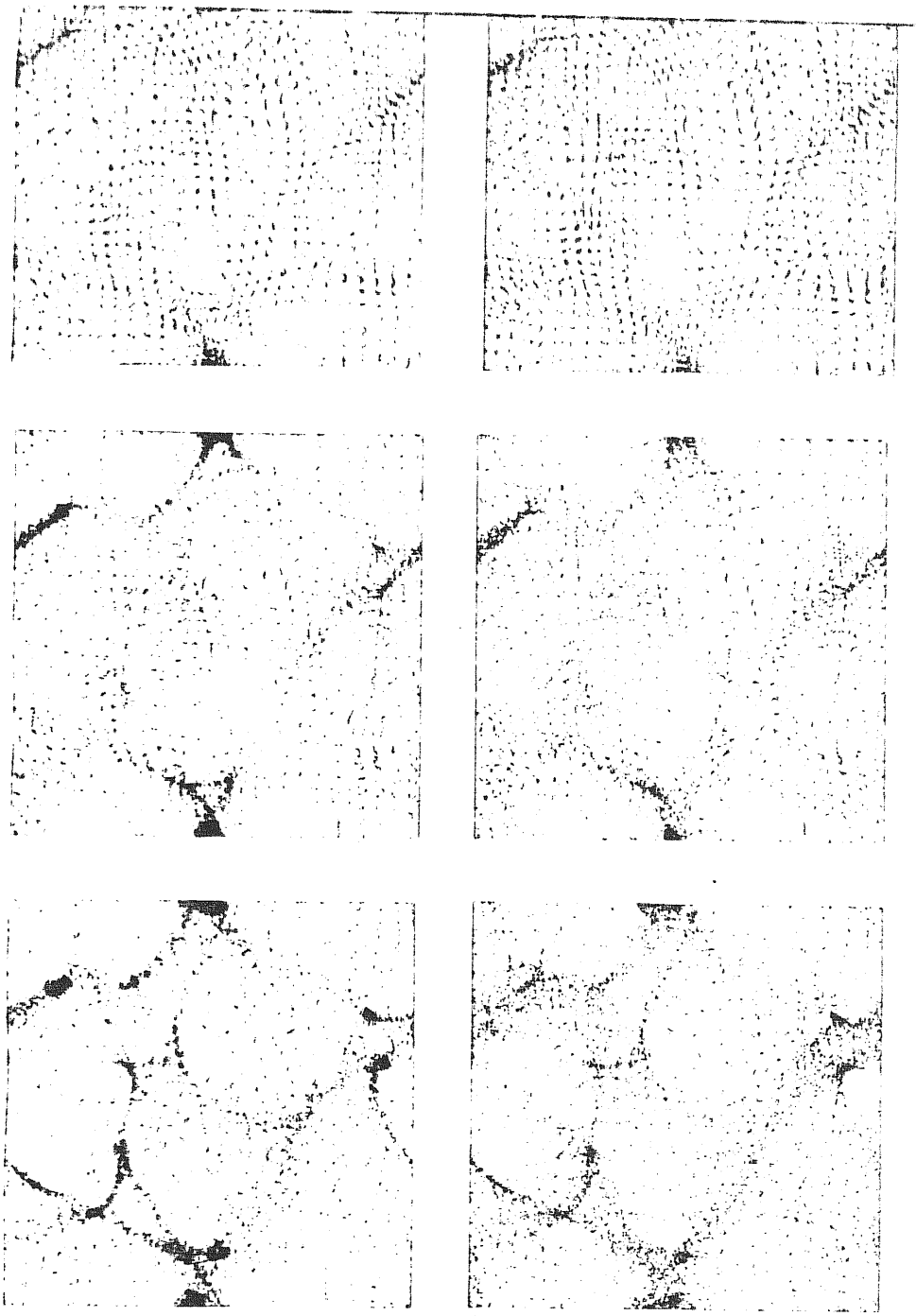

FIGURE 5.1 Comparison of the Zel'dovich approximation Eq. (5.18) with a numerical simulation of gravitational clustering using "pancake" initial conditions. The three rows show projections of the particle positions after the system had expanded by factors of 2.4, 3.6 and 5.4 respectively. Pictures to the left show the N-body simulation and pictures to the right show the Zel'dovich approximation.

temperature fluctuations are related to adiabatic fluctuations as(Silk 1981)

$$\frac{\delta T}{T} = \frac{1}{3}\left(\frac{\delta \rho}{\rho}\right)_{adia} \qquad (2.27)$$

The horizon size at recombination subtends 6° of arc on the sky. The corresponding scale to M_D^{adi} ($\sim 10^{12} - 10^{14}$) is 5' -10'. We expect then that the temperature fluctuations in the case of the adiabatic theory to be

$$\frac{\delta T}{T} \sim 10^{-3} \qquad \text{on these scales .} \qquad (2.28)$$

Infra-red observations at $\sim$ 600 micron wavelengths give variations over 6° as $\delta T/T \leq 3.5 \times 10^{-5}$. (Melchiori et.al. 1981). Patridge(1980) gives $\delta T/T \leq 10^{-4}$ for $\theta \geq 3'$. Table 2 summarizes a list of all the published upper limits on the small scale anisotropy of the MBR(Patridge 1983). We see from the table that the limits are uncomfortably tight for the adiabatic galaxy formation picture. Moreover we have seen that the perturbation spectrum is highly contrived unless $\Omega = 1$. (Silk and Wilson 1981 ; Wilson and Silk 1981 ; Peebles 1981).

The isothermal picture seems to have no problems of conflicting with the MBR. As the name itself suggests, these perturbations leave the photon density unaltered since these involve perturbations only in the matter density.
Under the assuption of a power-law spectrum of the isothermal fluctuations at the epoch of recombination we have seen that the characteristic masses are of the order $10^5 - 10^7 M_\odot$, comparable to the Jeans mass just after recombination

$$M_J \sim 10^5 (\Omega h^2)^{-1/2} M_\odot \qquad (2.29)$$

The first objects to condense out in this case are objects of masses $\sim M_J$. This mass corresponds roughly to that of a globular cluster.Subsequently, these objects will cluster under the action of gravity and build up structures of larger and larger scales, right upto the extent of superclusters. Since gravity alone is responsible for the generation of clustering and structure , there should be no characteristic scale of galaxy clustering.

We have seen that the two-point correlation function can be expressed as a power-law. The main aim of theoretical models is to calculate the expected correlation function and compare with observations, given the initial density fluctuation spectrum.

TABLE 2

Table 1

A list of all published upper limits on the small-scale anisotropy of the cosmic microwave background. The results are generally expressed as limits at the 95% confidence level. The corrections are my own estimates, and may be ignored.

Observ.	Wavelength cm	Angular scale	Reported or published upper limit $\Delta T/T$	Corrected upper limit $\Delta T/T$
1.	2.80	10′	1.8×10^{-3}	3.5×10^{-3} *
2.	0.35	2′	9.0×10^{-3}	2.0×10^{-2}
3.	0.35	~1.5	3.7×10^{-3}	1.8×10^{-3}
4.	3.60	2′–1°	7.0×10^{-4}	
5.	2.8	3′–1°	3.0×10^{-5}	4.0×10^{-4}
6.	4.0	~12′x40′	5.0×10^{-5}	1.6×10^{-4} *
7.	11.0	8′–20′	1.5×10^{-4}	4.0×10^{-4} *
8.	0.13	30′	1.2×10^{-4}	
9.	4.0	5′ to 150′	8.0×10^{-5} to 1.3×10^{-5}	4.0×10^{-4} to 7.5×10^{-5}
10.	0.9	~ 7′	8.0×10^{-5}	
11.	6.3	7′	$< 6\times10^{-4}$	
12.	2.8	11′	$< 2.5\times10^{-4}$	
13.	2.8	4.5	$< 2.5\times10^{-4}$	

* Converted to 2σ values and corrected for telescope efficiency. Not corrected for possible errors in statistical analysis.

1. Conklin and Bracewell (1967)
2. Penzias *et al.* (1969)
3. Boynton and Partidge (1973)
4. Carpenter *et al.* (1973)
5. Parijskij (1973a)
6. Parijskij (1973b)
8. Caderni *et al.* (1977)
9. Parijskij *et al.* (1977)
10. Partridge (1980b)
11. Ledden *et al.* (1980)
12. Seielstad *et al.* (1981)
13. Birkinshaw *et al.* (1981)

The isothermal picture for galaxy formation, known as the "hierarchical scenario" or the "bottom-up", should give the right clustering observed in the universe for an assumed initial spectrum. If all the galaxies are arranged in a nested hierarchy, Peebles(1974) has shown that the power index γ of $\xi(r)$ to be

$$\gamma = \frac{9+3n}{5+n} \qquad (2.30)$$

in the non-linear regime($\delta\rho/\rho >> 1$) . Peebles has suggested that $n=0$ initial spectrum is an appropriate fit to the observed $\xi(r)$. More extended calculations by Gott and Rees(1975) suggested that $n=-1$ spectrum gives a better fit to the overall $\xi(r)$ curve than $n=0$ spectrum for both $\Omega=1$ and $\Omega=0.1$. Hiyoshi and Kihara (1975) from N-body simulations for $\Omega=1$, found that $n<0$ is a good fit. Peebles and Davis(1977) using the BBGKY hierarchy equations found that $n=0$ is matches the observed $\xi(r)$ well.

A better answer to all this might come from detailed computer simulations. Using N-Body simulations Aarseth et.al.(1979) and Efstathiou and Eastwood(1981) for $n=0$ and $\Omega=1$ they found that the observed spectrum is too steep. Figure 8 shows projections of an $\Omega=1$ model with Poisson initial condition, that is, $n=0$

The isothermal picture of galaxy formation is promising but the mechanism to produce the perturbation is not yet found. In fact the recent ideas in particle physics suggest that the number of photons per baryons is frozen in from early epochs and should have a universal value(Weinberg 1981). This might preclude primordial isothermal fluctuations altogether.

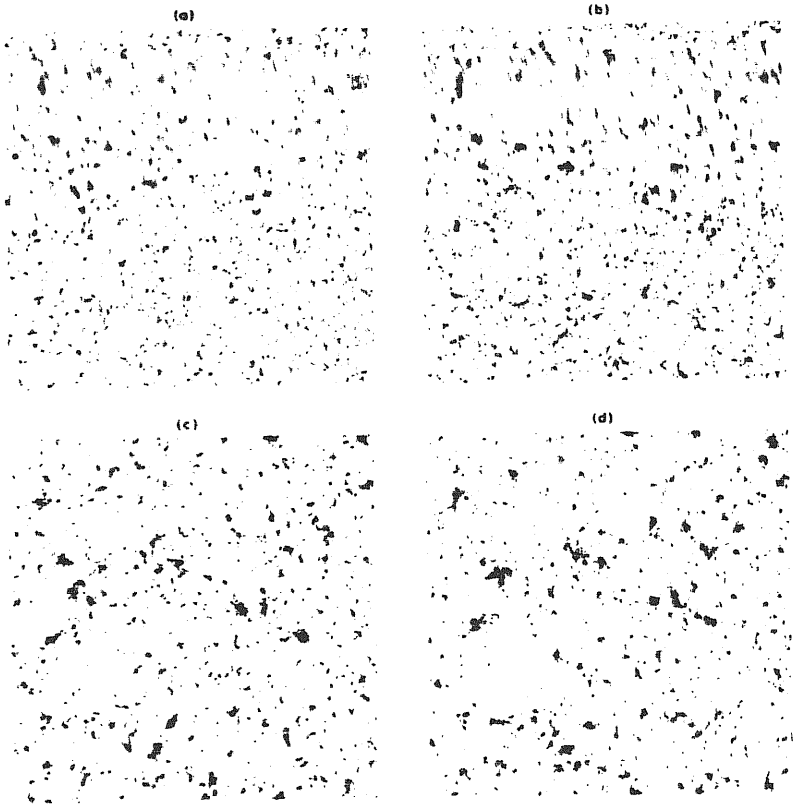

FIGURE 8

FIGURE 5.4 Evolution of clustering in a large N-body simulation ($N = 20{,}000$) with Poisson initial conditions and $\Omega = 1$. (a) Shows positions after the system has expanded by a factor of 5.1; (b) after expansion by a factor of 9.8; (c) after expansion by a factor of 16.0; (d) after expansion by a factor of 28.1.

CHAPTER THREE

GALAXY FORMATION WITH DARK MATTER

Recent advances in the grand unified theories of the strong, weak and electromagnetic interactions has provided a natural explanation for the observed entropy per baryon number, which is one of the fundamental numbers needed to characterize the Fridmann cosmological model, in terms of baryon non-conserving and CP violating processes, that occur in these theories. Several authors (Weinberg 1982; Press and Vishniac 1980) have made the important point that the entropy per baryon number is fixed in terms of purely microscopic parameters and should not vary from point to point in space. While the entropy per comoving volume remains constant, the baryon number, an excess of particles over anti-particles, which is initially zero, is generated as the symmetry of the grand unified era is broken, soon after the Planck time. Since a universal baryon number is generated , any pre-existing isothermal perturbations which are entropy variations cannot survive in the standard model. Only adiabatic perturbations survive and should be present to form galaxies.

We have seen that galaxy formation in the adiabatic case, the pancake scenario, is difficult to reconcile with observations of microwave background , the spatial distribution of galaxies and the light element abundances, unless $\Omega \approx 1$ and the perturbation spectrum is highly contrived. But $\Omega \approx 1$ baryon dominated universe is in conflict with the upper limits to the baryon density($\Omega_b \leq 0.1$) inferred from the big-bang nucleosynthesis(Yang et.al. 1984). On the other hand , we have seen that evidences based upon dynamical arguments suggest that $\Omega > 0.1$, perhaps as high as $\Omega \sim 1$, implying the existence of dark matter(DM), having a density greater than Ω_b . Since this DM is found to be dominating gravitationally on all scales larger than galaxy cores and amounts to some 90 percent by mass in the universe, it is likely that it plays an important role in galaxy formation.

A substantial fraction of DM surrounds the visible portions of galaxies. The following picture can be made for a galaxy; a dense, luminous core containing the stars, gas and other baryonic matter, surrounded by an invisible halo of DM, ten times larger in radius and containing 90 percent of the mass. When galaxies cluster, their halos probably merge, creating a fairly uniform sea of background DM, in which the luminous portions are embedded. The separation of baryonic matter, from DM on galaxy scales might probably be explained by the dissipational property of the baryons . Because when the baryonic matter is gaseous, it radiates, loses energy and sinks lower, while DM which interacts gravitationally only, does not radiate and a structure composed of

such matter collapses only a factor of roughly two or less from its point of maximum expansion. Therefore, DM is necessarily of some form of dissipationless matter. Since we have seen that the DM cannot be any of the conventional forms , let us consider the exotic choices particle physics has provided us.

3.1 HOT, WARM AND COLD DARK MATTER

Particle physics has provided a very long list of weakly interacting particle species, most of them hypothetical, whose relic abundance can supply the mass density contributed by the dark matter. The many candidates suggested, spanning an embarrassingly large mass range is given in the below table.

CANDIDATE	MASS	ABUNDANCE
Axion	$\sim 10^{-5}$ ev	$\sim 10^{9}$ cm^{-3}
Neutrino	$\sim$ 30 ev	$\sim$ 100 cm^{-3}
gravitino / Photino	$\sim$ 1 kev	few cm^{-3}
Sneutrino	$\sim$ 1 Gev	$\sim 10^{-6}$ cm^{-3}
Photino	$\sim$ 1 Gev	$\sim 10^{-6}$ cm^{-3}
Superheavy monopoles	$\sim 10^{16}$ Gev	$\sim 10^{-22}$ cm^{-3}
Primordial black-holes, jupiters etc	$\gg 10^{15}$ g $\approx 10^{39}$ Gev	$\ll 10^{-45}$ cm^{-3}

Of these various possibilities, only rocks, Jupiters and neutrinos have been directly observed, though a non-zero rest mass for the neutrino has not yet been confirmed. The viability of the other candidates is uncertain in two ways: first, they must be proved to exist in nature and, second they have to have a mass which matches their present number density in such a way as to produce the observed Ω.

Inspite of the long list of candidates with the different masses, some gereral themes have emerged. First, it is useful to classify these DM candidates. An useful classification scheme was introduced by J.R.Bond . In this scheme, the candidates are termed "hot", "warm" or "cold" dark matter according to their initial random velocities, relative to the comoving ,expanding co-ordinate frame of the universe.

The hot DM refers to particles that are light($\sim$ 100 eV) and which are relativisti at the time of their decoupling,and remain relativistic until shortly before they become the dominant matter in the universe. At that time, the temperature of the universe would be below their rest mass and they begin to cluster. The most popular candidate for the hot DM is the neutrino.

The warm DM are 10-100 times heavier than the hot DM with masses usually in the range 1-10 Kev and which decouple earlier than the hot DM and hence become non-relativistic early. An early candidate for the warm DM was the gravitino (G.R.Blumenthal et.al.1982) but recent changes in the scale of the supersymmetry breaking predict gravitinos to be more massive(100GeV), making it a candidate for the cold DM, and not a warm DM. A photino of 1KeV is a likely candidate but recent theories predict (Goldberg 1983) photinos to be more massive. At present there is no natural warm DM candidate.

Cold DM candidates are either very heavy particles that become non-relativistic at very early stage(gravitinos, photinos, right-handed neutrinos) or are particles that are born with intrinsically zero velocities(axions).

We shall see that the crucial cosmological distinction amongst these different types of elementary particles is the different role which collisionless damping plays in determining the structure which emerges in a universe dominated by one or the other of these particles. The nature of the structure which emerges out, is fully determined by the amplitude and shape of the adiabatic perturbation power spectrum as measured in the linear stage of growth , the post-recombination epoch(Doroshkevich et. al.1981, Bond et. al.1980,Wasserman 1981; Bond,Szalay and Turner 1982; Peebles 1982,1983; Turner,Wilczek and Zee 1983; Primack and Blumenthal 1983).

3.2 GALAXY FORMATION WITH HOT DM

The standard hot DM candidate is the massive neutrino(Doroshkevich 1981; Bond et.al. 1980). We know that a neutrino exists and there is no compelling reason to suppose that it is massless. In certain grand unification theories , the neutrino,which is one

component of a multiplet with its charged lepton and quark partners, attains a mass naturally . Witten(1980) and Gershtein and Zeldovich(1966) first realized that a neutrino with a small rest mass might lead to a gravitationally dominating overall neutrino density and they deduced a limit $m_\nu \leq 140$ ev for it from the age of the universe. Marx and Szalay(1972) and Cowsik and McClelland (1972) suggested massive neutrinos as possible candidates for the "missing mass" in the halos of galaxies. For many yaers, massive neutrinos were considered plausible but not compelling candidates for the DM , while the favoured scenarios were with ordinary nucleonic matter(faint stars, gas clouds etc.).

Primordial nucleosynthesis arguments(Yang et.al. 1984), ($\Omega_b < 0.034$) the need to explain the observed $\Omega \geq 0.15$, as indicated by dynamical arguments implying the need for DM, favoured neutrinos to other nucleonic scenarios. Experimental evidence for neutrino masses(Lyubimov et.al. 1980), as well as theoretical work in GUTS stimulated interest in neutrinos. A new trend was initiated by Szalay and Marx (1976) who noticed that the perturbation growth of neutrinos starts long before the decoupling of matter and radiation and that seems to provide an answer to the problems faced in the adiabatic case of galaxy formation. At present there is apparently no reliable experimental evidence for a non-zero neutrino rest mass. The Lyubimovet.al. (1980) measurement of the tritium beta-decay spectrum has suggested that the mass of the neutrino(electron) can be as large as 14-46 eV. Preliminary evidence for neutrino oscillations on the other hand, which implied a neutrino mass greater than $\sim$ 1eV(Reines et.al. 1980) has been called into question by Kwon(1981). Experiments have been reported,which claimed to place upper limits of 560 KeV and 250MeV to the masses of the μ and τ neutrinos respectively (Daum et.al. 1978). Recent studies of double beta decay have given model-dependent upper limits to the mass of the electron neutrino as $m_{\nu e} \leq 5.6$ ev (Kirstein et.al. 1983) and $m_{\nu e} \leq 10$ ev (Avignone et.al. 1983). In short the experimental evidence for a non-zero rest mass is extrememy uncertain and on the other hand the range of possibilities allowed by the grand unified theories which predict finite mass for a neutrino is great. We shall see how cosmology in principle , limits the sum of the masses of stable neutrino types to roughly 100eV(Schramm and Steigman 1981).

THE MASS CONSTRAINTS

During the early evolution of the universe, all particles including neutrinos, were produced copiously. Most of the neutrinos present in the universe today were produced

at the same time as most of the photons in the 2.7°K background radiation(Weinberg 1972). The neutrinos and anti-neutrinos (with masses $\lesssim$ 1MeV) are in thermal equilibrium with the photons and the electron-positron gas at T = 10^{10}K ($\sim$ 1MeV) Their mean occupation no. as a function of momentum p and time t is given by the non-degenerate Fermi-Dirac (FD) distribution of extreme relativistic(ER) particles.

$$n(p,t) = \left[1 + \exp \frac{\sqrt{m_\nu^2 + p}}{kT}\right]^{-1} \approx \left[1 + \exp (p/kT)\right]^{-1} \qquad (3.1)$$

since $m_\nu \ll kT \approx$ 1MeV.($\hbar = c = 1$).
This equation is valid even in the non-relativistic (NR) regime where neutrinos are neither FD nor degenerate. The neutrinos remain in thermal equilibrium until the temperature drops to $T_{\nu d}$, at which point their mean free path exceeds the horizon and they essentially cease interacting thereafter except gravitationally.
The neutrino mean free path is

$$\lambda_\nu \sim (\sigma_\nu n_{e^\pm})^{-1} \qquad (3.2)$$

where σ_ν denotes the cross-sections for neutrino-antineutrino reactions and $n_{e^\pm}$ is the density of charged leptons .

$$\sigma_\nu \approx g_{wk}^2 \hbar^{-4} (kT)^2 \quad \text{for} \quad kT < m_\mu \qquad (3.3)$$

where $g_{wk} = 1.4 \times 10^{-49}$ erg cm^3 is the weak coupling constant, known from the observed rate for the muon decay process $\mu^+ \rightarrow e^+ + \nu_e + \bar{\nu}_\mu$
The density of the charged leptons $e^\pm$ is given by

$$n_{e^\pm} \approx \left(\frac{kT}{\hbar}\right)^3 \qquad (3.4)$$

Taking $\hbar = c = 1$, we have the neutrino mean free path from the above equations as

$$\lambda_\nu \sim (\sigma_\nu n_{e^\pm})^{-1} \sim \left[(g_{wk}^2 kT)^2 \times (kT)^3\right]^{-1} \sim$$

$$\sim \left[(g_{wk}^2 T^2)(T^3)\right]^{-1} \qquad (3.5)$$

The horizon size at that time is

$$\lambda_H \sim (G\rho)^{-1/2} \sim G^{-1/2} \rho^{-1/2} \sim M_{Pl} T^{-2} \qquad (3.6)$$

where $M_{Pl} \equiv G^{-1/2} = 1.22 \times 10^{19}\ GeV = 2.18 \times 10^{-5}\ g$ is the Planck mass.

Thus

$$\lambda_H/\lambda_\nu \sim \frac{(g^2_{wk} T^2)(T^3)}{T^2} M_{Pl} \sim \left(\frac{T}{T_{\nu_d}}\right)^3 \qquad (3.7)$$

with the neutrino decoupling temperature

$$T_{\nu_d} \sim g_{wk}^{-2/3} M_{Pl}^{-1/3} \sim 1\ MeV \qquad (3.8)$$

When the temperature of the universe falls below 1MeV, $e^+ e^-$ annihilation ceases to be balanced by pair creation and the entropy of the $e^+ e^-$ pairs heats the photons. At temperatures above 1MeV, the number of neutrinos $n_\nu = \frac{3}{4} n_\gamma$, where the factor $3/4$ comes from Fermi vs. Bose statistics. But the $e^+ e^-$ annihilation increases the photon number density relative to that of the neutrinos by a factor $11/4$. Thus, today, the number of neutrinos (plus antineutrinos) of each type present in the universe is

$$n_{\nu_0} = \frac{3}{4} \cdot \frac{4}{11} \cdot n_{\gamma_0} = 109\ cm^{-3} \qquad (3.9)$$

Subscript zero here indicates the present epoch, again.

n_{γ_0} is the number of black-body photons observed today. It is given by

$$n_{\gamma_0} = 8\pi \left(\frac{kT}{hc}\right) 2\, \zeta(3) = 399\ cm^{-3} \qquad (3.10)$$

with $T = 2.7^\circ K$, $\zeta(3) = 1.020206$.

The present cosmological density is

$$\rho \equiv \Omega \rho_c = 11\, \Omega h^2\ KeV\ cm^{-3} \qquad (3.11)$$

Therefore it follows from the above that

$$\sum_i m_{\nu_i} < \frac{\rho}{n_{\nu_0}} \leq 100\, \Omega h^2\ eV \qquad (3.12)$$

where $\sum_i m_{\nu_i}$ is the sum of all the neutrino species with $m_{\nu_i} \leq 1MeV$. Consistency with the widest range allowed as well as the restrictions of $\Omega < 3$ and $h > \frac{1}{2}$ gives

$$\sum_i m_{\nu_i} \leq 100\ eV \qquad (3.13)$$

In general the sum of the masses for different neutrini types should have to satisfy this relation. The required mass range is compatible with the experimental upper limits for the masses of ν_μ and ν_τ and also for ν_e if $h \leq 0.7$.

Similar constraints can also be found on the masses of other fermions which decouple while still relativistic and are candidates for the DM ; the analysis differs only in the decoupling temperature and in the number of spin states available to the fermion (K.A.Olive and M.S.Turner 1982; Bond and Szalay 1983). The particles decoupling earlier at higher temperatures miss the heating due to annihilation of $\mu^+\mu^-$ or other species and thus have lower temperatures given by

$$T_f = T_\gamma \left[\frac{3.9}{g_{*f}} \right]^{1/3} \qquad (3.14)$$

Here f stands for any hypothesized fermion particle which decouples when it is relativistic; g_{*f} is the number of relativistic species at decoupling(K.A.Olive et.al. 1981). The FD number density for particles which decouple while still relativistic is

$$n_f = \frac{3 g_f T_f^3}{4\pi^2} \zeta(3) = \frac{3 g_f T_\gamma^3}{4\pi^2} \zeta(3) \left(\frac{3.9}{g_*} \right) \qquad (3.15)$$

g_f = spin degrees of freedom(2 for spin ½ partners like photinos and neutrinos) and $\zeta(3) = 1.020206$. The energy density of a fermion species of mass m_f is given by

$$\Omega_f = \frac{m_f}{97\ eV} h^2 \left(g_f/2 \right) \left(\frac{10.75}{g_{*f}} \right) \left(\frac{T_{\gamma_0}}{2.7\ K} \right)^3 \qquad (3.16)$$

For a particle of decoupling temperature

$$\geq \begin{bmatrix} 100\ MeV \\ 500\ MeV \\ 100\ GeV \\ 10^{14} \end{bmatrix}, \quad g_* = \begin{bmatrix} 14.5 \\ 61.8 \\ 104 \\ 161 \end{bmatrix} \qquad (3.17)$$

$$\Omega_f = m_f \begin{bmatrix} 130 \\ 560 \\ 940 \\ 1450 \end{bmatrix}^{-1} \cdot h^{-2} \cdot \left(g_f/2 \right) \cdot \left(\frac{T_{\gamma_0}}{2.7\ K} \right)^3 eV$$

Consistency with the "best fit" range of ages($t_u > 6$ yr from globular clusters), restricts

$$\sum_f m_f \leq \begin{bmatrix} 32 \\ 140 \\ 230 \\ 360 \end{bmatrix} \left(2/g_f\right) \text{ eV}$$

For all standard unified models with $g_{*f} \leq 161$, m_f cannot exceed 400eV. Thus, we see that the big bang cosmology puts stringent limits on the number of types and masses allowed for the particles.

THE CHARACTERISTIC SCALES

Collisionless particles have no pressure but they still have kinetic energy from their thermal motion. So one can define an effective Jeans length and mass for these particles by using the velocity dispersion $\frac{1}{3}\langle v^2 \rangle$ instead of c_s^2 in the expression for the Jeans mass. As usual, perturbations on mass scales M greater than M_{J_f}, the effective Jeans mass for the hot DM, grows, while those on smaller scales do not, since particles stream out of density fluctuations on times which are shorter than the local gravitational time scale $t \sim (G\rho)^{-1/2}$. In the comoving frame, when the random particles are relativistic, $M_{J_f} \sim M_H$, since the horizon size and free-streaming length are comparable. M_{J_f} thus increases proportionally to t, the age of the universe(Bond et.al. 1980). Fig. 9 shows the growth of M_{J_ν} for the neutrinos.

When the particle velocities become non-relativistic, M_{J_f} decreases with time. Hence, the Jeans mass reaches a maximum M_J^{max} roughly when $kT_f \sim m_f c^2$, where T_f is the kinetic temperature corresponding to the particles of mass m_f, after which the M_{J_f} begins to decrease. The mass which fills the horizon at the time of transition from relativistic to non-relativistic particle velocities ($kT_f \sim m_f c^2$) is

$$M_H\left(kT_f \sim m_f c^2\right) \approx g_f\, M_{Pl}^3\, m_f^{-2}\, \alpha^6 \qquad (3.18)$$

where $\alpha = T_f/T_\nu$ is the factor which gives the "heating" of the photons relative to the fermion particles, from annihilations of other species after the decoupling of these particles.

The transition from radiation to matter domination occurs at redshift z_{eq}

FIGURE 9

FIG 5

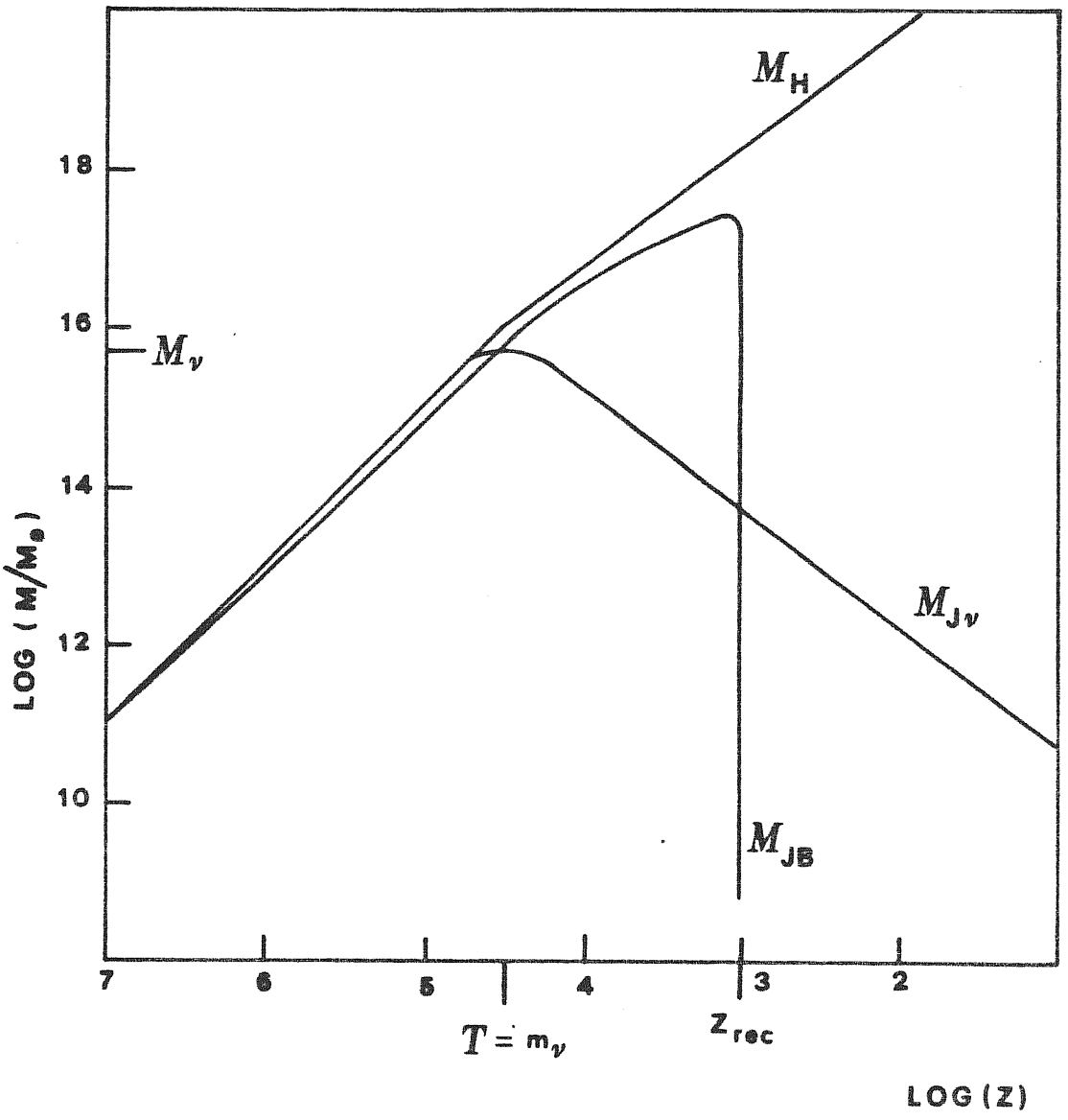

$$(1+z_{eq}) \approx 4 \times 10^4 \Omega h^2 \qquad (3.19)$$

The mass M_{eq} which fills the horizon at this epoch is

$$M_{eq} \gtrsim 10^{15} (\Omega h^2)^{-2} M_\odot \qquad (3.20)$$

Since $M_{Jf}^{max} \sim M_H(kT_f \sim m_f c^2)$,the effective Jeans mass for these particles is just the mass which fills the horizon at z_{eq}

$$M_{Jf}^{max} \sim M_{eq} \qquad (3.21)$$

For example, in the case of neutrinos of non-zero mass , $m_\nu \approx 30eV$, the distance travelled during the transition from relativistic to non-relativistic state is (Bond et.al. 1980; ,Sato and Takahara 1981),

$$d_\nu = \lambda_H (kT \sim m_\nu c^2) \sim M_{Pl} m_\nu^{-2}$$
$$\sim 41 (m_\nu / 30\,eV)^{-1} (1+z)^{-1} \text{ MPC} \qquad (3.22)$$

In order to survive this free streaming, a neutrino fluctuation must be larger in linear dimension than d_ν . Correspondingly, the Jeans mass $M_{J\nu}$ is given by

$$M_{J\nu} \approx 1.77 M_{Pl}^3 m_\nu^{-2} = 3.2 \times 10^{15} (m_\nu / 30\,eV) \qquad (3.23)$$

THE SHAPE OF THE PERTURBATION SPECTRUM

In order to see what non-linear structure emerge, we must consider the shape of the perturbation spectrum

$$\frac{\delta\rho}{\rho} \propto M^{-(n-1)/6} \qquad (3.24)$$

The most salient feature of the hot DM is the erasure of small fluctuations by free-streaming. Free-streaming eliminates power in the perturbation spectrum for all scales $M < M_J^{max} \sim M_{eq}$. The spectrum on scales $M > M_J^{max} \sim M_{eq}$, retains its shape, transformed to

$$\frac{\delta\rho}{\rho} \propto M^{-(m+3)/6} \qquad (M > M_{eq}) \qquad (3.25)$$

for all the mass scales M which have entered the horizon.

Since $M_{eq} \gtrsim 10^{15}(\Omega h^2)^{-2} M_\odot$,scales of the order of superclusters are the first objects to form in a hot DM dominated universe. These are the pancake masses referred to earlier. Small scale structures like galaxies can form only after the initial collapse of these supercluster size fluctuations through fragmentation (Shapiro 1983).

GROWTH OF FLUCTUATIONS

The growth of a fluctuation, of M vs z in the universe is shown in Fig. 10 , for three different cosmological scenarios.

$$(i)\ \Omega_\nu = 0\ ,\ \Omega_B = 0.03\ ;\ (ii)\ \Omega_\nu = 0\ ,\ \Omega_B = 1\ ;\ (iii)\ \Omega_\nu = 1\ ,\ \Omega_B = 0.03$$

The dashed line corresponds to the neutrinos;the three solid lines show the growth of baryon fluctuations in the three different cases.
In the case of(i) $\Omega_\nu = 0$, $\Omega_B = 0.03$, $\frac{\delta T}{T}$ is very small $\cong 3\times 10^{-5}$.
As we have seen before (ii) $\Omega_\nu = 0$, $\Omega_B = 1$ gives $\frac{\delta T}{T} \simeq 10^{-3}$,which is too large to be consistent with the MBR fluctuations . In the case of $\Omega_\nu = 1$, $\Omega_B = 0.03$, the growth of $\left(\frac{\delta\rho}{\rho}\right)_{baryon}$ is first inhibited by the large radiation density(Meszaroe 1974), then by the Ω^{-1} effect. The fluctuation growth from $z = 10^3$ to $z = 0$ is only ~ 15 ; $\frac{\delta T}{T} \cong 0.06$ in this case.

The absence of the small angle $\frac{\delta T}{T}$ fluctuations in the case of a neutrino dominated universe, makes it a very attractive picture for galaxy formation.

GALAXY FORMATION IN HOT DM UNIVERSE

Galaxy formation in a hot DM dominated universe falls within the context of the pancake scenario. Several calculations have been done by various authors (Shapiro et.al. 1983; Centrella and Melott 1983; Klypin and Shandarin 1983; Frenk et.al.1983), taking the case of a neutrino dominated as the prototype for the universe dominated by hot DM. The calculation involves two parts: (i) the structure which evolves

FIGURE 10

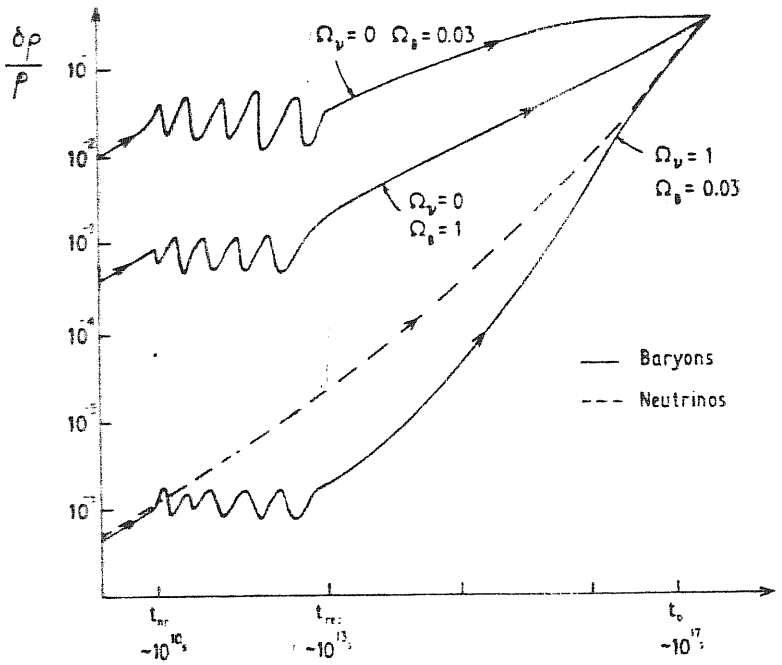

FIGURE 15 Typical growth tracks of density perturbations versus time in Universes of different baryon density. The solid lines track the growth of baryon inhomogeneities and the dashes a neutrino inhomogeneity. The microwave background inhomogeneities are imprinted at recombination, prior to which the baryon inhomogeneities undergo a period of oscillation whilst the neutrino inhomogeneity amplifies continuously, (Doroshkevich *et al.*, 1982).

in the neutrino dominated universe; (ii) the fragmentation and the galaxy formation. The first part involves collisionless particle numerical simulations, of the growth of the appropriate linear perturbation spectrum into the non-linear stage. The second involves detailed, numerical hydrodynamical calculations of the coupled growth of the baryon and neutrino perturbations into the non-linear stage, including the effects of ionization, recombination, radiative and compton cooling and thermal conduction.

Many calculations have been performed (previous references) of the 3-dimensional collisionless, gravitational clustering of the neutrinos in the post-recombination Friedmann universe, starting with the perturbation spectrum appropriately peaked at wavelength $\lambda \simeq d_\nu$. Fig. 11 shows the 2-dimensional simulation of such a calculation (Melott 1983). In the numerical simulations, the regions of high density formed a network of filaments, with the highest densities occurring at the intersections (knots) and with voids inbetween. The similarity of these features to those seen in the observations is the most attractive feature of the hot DM. In fact, the most serious problem of the other DM (warm and cold) is the failure to produce this large scale structure seen in the universe. Another attractive feature of this picture is the advantage in explaining the important Hubble-type environment correlations.

PROBLEMS WITH HOT DM

In spite of the attractive features, the lack of small angle $\frac{\delta T}{T}$ fluctuations, the formation of filaments, voids, the Hubble-type environment correlations, a number of serious problems with the hot DM have emerged in the recent studies.

(1) Studies of non-linear clustering ($\lambda < 10$ Mpc) (S.D.M.White et. al. 1983) have shown that the supercluster collapse must have occurred recently, at redshift $z_{sc} < 2$! This was also consistent with a study of streaming velocities in the linear regime($\lambda > 10$ Mpc), which indicated that $z_{sc} < 0.5$ (Kaiser 1983). However, the best limits on galaxy ages from globular clusters, plus the possible association of QSOs with galactic nuclei and their abundances at $z > 2$, indicates that galaxy formation took place before $z = 3$. This is inconsistent with the neutrino picture for galaxy formation, in which superclusters form before galaxies: $z_{sc} > z_{galaxies}$.

(2) A second serious problem is the ratio of the total to baryonic matter, M/M_b , on large and small scales. Large clusters($10^{15}\ M_\odot$) have higher internal velocity dispersions than galaxies. Galaxies fragmenting within clusters will therefore be able to capture only the more slowly moving hot DM particles, and the DM halos

FIGURE 11

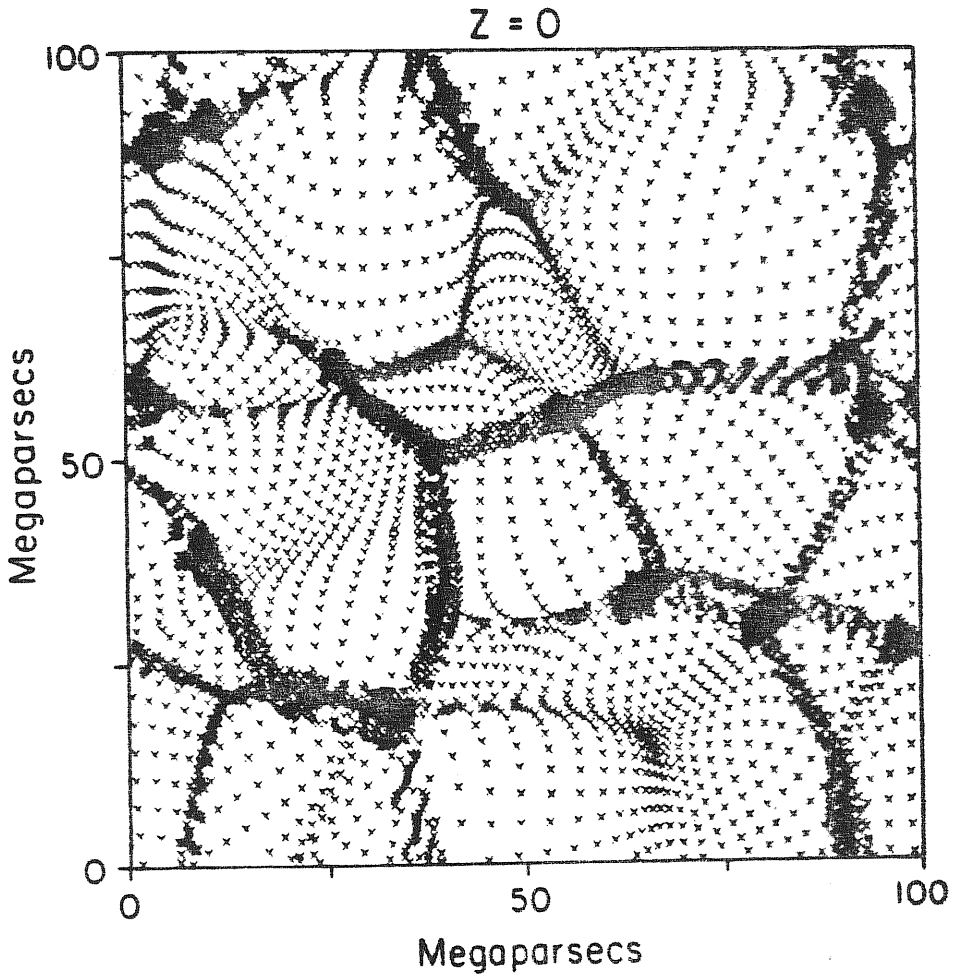

FIG. 1.—The location of 10,000 sample points (of the 90,000) particles at $Z = 0$. The 1 Mpc grid is the size of the ×'s in the illustration, which covers the whole field of the simulation. We show the particle from every third row and column of the initial array, or one-ninth of the particles, so as not to overwhelm the eye.

around galaxies will consequently be reduced in mass. 1-dimensional numerical simulations predict that the ratio M/M_b ~ 5 times larger for clusters than for galaxies ($\sim 10^{12} M_\odot$) (Bond et.al. 1983), since the larger clusters with their higher escape velocities are able to trap a considerably larger fraction of the hot DM particles. While there is evidence that the M/L ratio increases with scale there is also evidence that the more meaningful ratio of total to luminous mass M/M_{lum} remains constant, from large clusters through groups of galaxies, binary galaxies and ordinary spirals. See fig. 12 and table 3 (Faber 1983). The M/M_{lum} of rich clusters is similar to that of galaxies including their massive halos, even though M/L for clusters is larger. This is mainly because of the different stellar populations in the ellipticals in rich clusters and the large contribution of X-ray emitting gas to M_{lum}. The table suggests that there is no significant evidence for an increase in M/M_b from galaxies to clusters , in conflict with the numerical results.

(3) A serious blow to the hot DM picture comes from the recent theoretical arguments (Lin and Faber 1983) and observational evidence from the velocity dispersion data for Draco, Carina and Ursa Minor (Aaronson 1983; Lin and Faber 1983) that dwarf spheroidal galaxies hava substantial amounts of dark matter. If this dark matter consists of weakly interacting particles of rest mass m_ν, then Liouville's theorem implies that (Tremaine and Gunn 1979, Peebles 1982)

$$m_\nu > 10^2 \left(\frac{100 \text{ Km sec}^{-1}}{\sigma}\right)^{1/4} \left(\frac{1 \text{ KPc}}{r_c}\right)^{1/4} \text{eV} \qquad (3.26)$$

where σ is the 3-d velocity dispersion of the particles and r_c is the core-radius of the particle distribution. For Draco, with $\sigma \sim 10$ Km sec^{-1} and if one takes for r_c the observed tidal radius of 500 pc (Hodge 1971), we get

$$m_\nu \geq 240 \text{ eV} \qquad (3.27)$$

A similar argument for spiral galaxies (our galaxy) would imply $m_\nu > 30$ eV. This phase space constraint puts another limit to the allowed range of masses for the dark matter.

Aaronson (1983), using a smaller value of r_c for Draco, finds $m_\nu \geq 530$ eV , which is certainly incompatible with the cosmological constraint given by equation 3.13. However, the present velocity dispersion estimates are uncertain and further observations are needed to confirm the result,before a serious dilemma is assumed to exist for

FIGURE 12

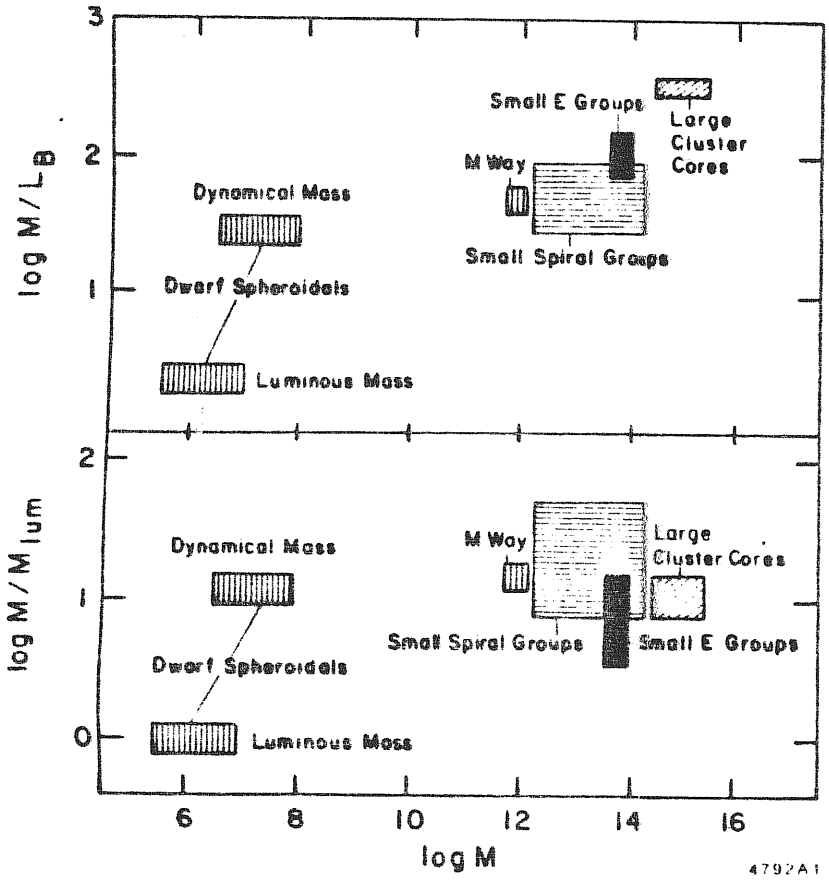
log M/L_B
log M/M_lum
log M
Small E Groups
Large Cluster Cores
M Way
Small Spiral Groups
Dynamical Mass
Dwarf Spheroidals
Luminous Mass
Large Cluster Cores
Small E Groups
3
2
1
0
6
8
10
12
14
16
4792A1

TABLE 3

Table 1

The Ratio of Total to Baryonic Matter on Various Mass Scales[a)]

Structure	Mass Scale M	Mass-to-Light M/L	Total-to-Baryonic Mass M/M_B	% Hot Gas
Large clusters	$10^{15}\ M_\odot$	316±40	8.4±1.1	84
Small E-dominated groups	5×10^{13}	83±6	5.4±0.5	61
Small spiral-dominated groups	2×10^{13}	40^{+50}_{-16}	14.2^{+36}_{-6}	0:
Entire Milky Way	10^{12}	50	14	0:

a) Details to appear in Blumenthal, G.R., Faber, S.M., Primack, J., and Rees, M., in preparation, 1984.

the hot DM pancake scenario. But the phase-space constraints and the indications of DM in dwarf spheroidals, led several authors(Sciama 1982; Cabbibo et.al. 1981) to consider photinos, the spin ½ supersymmetric partners of the photons($m > 500\ eV$) to be the dominant matter in the universe. They come under the category of warm DM, which will be discussed next.

Besides these problems with the hot DM, the picture also needs a well-defined theory for the fragmentation process of the protoclusters, which at present, is not very clear.

3.3 GALAXY FORMATION WITH WARM DM

Warm dark matter consists of particles which interact more weakly than the hot DM and decouple at temperatures $T_{wd} >> T_{hd}$ while still relativistic. Because of their early decoupling, their number density is not increased by particle annihilation at temperatures below T_{wd} (subscript " w " standing for warm DM particles).
One suggestion for a warm DM particle was the ~ 1 KeV gravitino, the spin $^3/_2$ supersymmetric partner of the graviton (Pages and Primack 1982),but recent changes in the scale of supersymmetry brea king (Savoy 1983) now predicts a mass of 10^2 GeV for the gravitino, which does not make it a candidate for warm DM. Another suggestion for a warm DM particle was the photino,the spin ½ supersymmetryc partner of the photon (Sciama 1983), with mass $m_{\tilde{\gamma}}$ greater than 500 eV and $T_{wd} \sim$ 200 MeV.
But with the current models of supersymmetry and the requirement that the photinos almost all annihilate (Weinberg 1983; Goldberg 1983),so that they do not contribute too much to the mass density,we have $m_{\tilde{\gamma}} \gtrsim 2\ GeV$ (ref.as before).
At present there is no suitable warm DM particle,unlike hot and cold cases;but they cannot be excluded.

With the standard assumpion of entropy conservation per comoving volume,the number density n_{w_0} of warm particles today,and their mass m_w can be calculated in terms of the effective number of helicity states of interacting bosons (B) and fermions (F) (Steigman 1976; Primak 1983)

$$g_*(T_{wd}) = g_B + \frac{7}{8} g_F \qquad (3.28)$$

The current standard model of particle physics ,together with the simplest grand unified theories (minimal SU(5)),predict $g_*(T) \sim 10^2$ for T between 10^2 GeV

and $T_{GUT} \sim 10^{14}$ GeV, with only a factor unity increase in $g_*(T)$ from supersymmetric particles. Then for T_{wd} in the range 1 GeV — 10^{14} GeV, we have (Primak 1983)

$$n_{w_0} \simeq 5\, g_w \ cm^{-3}$$

$$m_x \simeq 2\, \Omega h^2\, g_w^{-1} \ KeV$$

where g_w is the number of helicity states.

Unlike the hot case, the transition from relativistic to non-relativistic particle velocities for these warm particles occur significantly earlier than the transition from radiation to latter domination in the universe. Therfore the Jeans mass M_{J_w} for these particles is significantly smaller than M_{eq}. The Jeans mass M_{J_w} for particles of masses $m_w \sim 1$ KeV is

$$M_{J_w} \sim 10^{12}\, M_\odot (\Omega h^{-2}) \ll M_{eq}$$

which the scale of a large galaxy (see fig. 13).

THE FLUCTUATION SPECTRUM

The fluctuation spectrum which results from the effects of damping on the primordial spectrum in the case of warm dark matter is different from the hot DM case. Once again, all the power $M < M_{J_w}$ is damped away and as before the primordial shape is

$$\frac{\delta\rho}{\rho} \propto M^{-(n+3)/6} \quad \text{for} \quad M > M_{eq} \qquad (3.29)$$

The scales which come across the horizon between M_{J_w} and M_{eq} are however supressed by radiation, which still dominates, unlike in the hot DM, where $M_{J_\nu} \sim M_{eq}$. As a result, the spectrum is flattened relative to eqn. (3.29) to

$$\frac{\delta\rho}{\rho} \propto M^{-(n'+3)/6} \quad (M_J \lesssim M \lesssim M_{eq}) \qquad (3.30)$$

Where $n' \cong n-3$. This means that the warm DM has a power over an increased range of masses, roughly from $10^{11}\, M_\odot$ to $10^{15}\, M_\odot$. The first non-linear structure to form in the case of warm DM is roughly of order of galaxy scales, and galaxy formation here proceeds according to the hierarchical scenario.

FIGURE 13

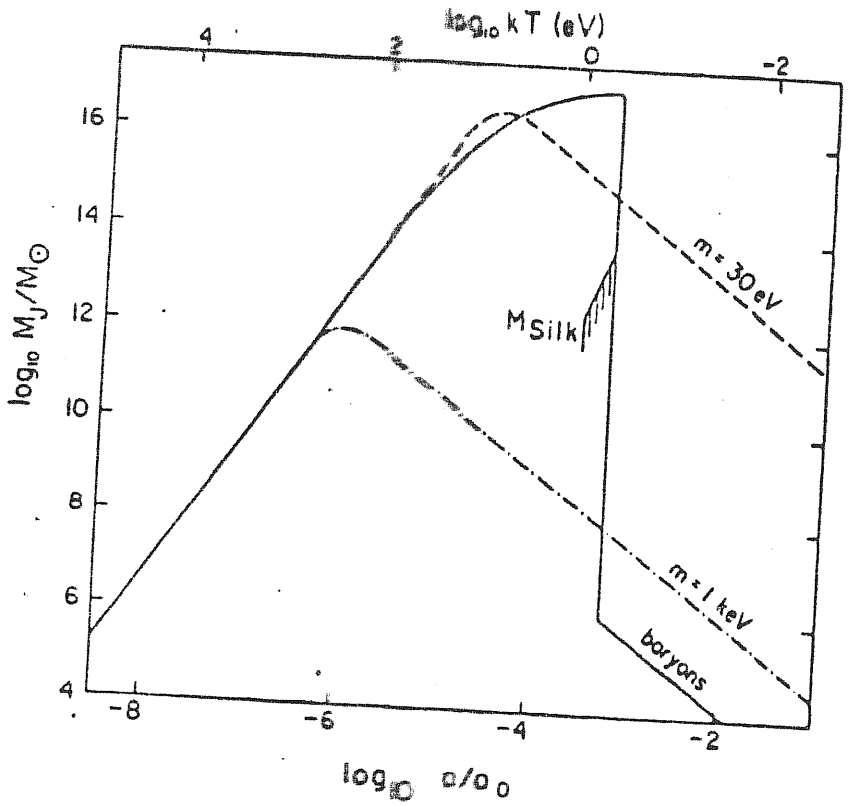

Figure 3. The Jeans mass versus scale factor for a baryon, hot DM(m = 30 ev), and warm DM (m = 1 keV) dominated universe with $\Omega h^2 = 1$. Hot and warm DM perturbations with $M < M_J$ at any time are dissipated by free-streaming.

PROBLEMS WITH WARM DM

Since galaxies collapse first, the problem of galaxies forming very late does not come up in the warm DM case. Galaxies also have not to accrete their dark halos via fragmentation within a larger structure, so no trend is expected in the total to barion ratio M/M_b above $10^{12}\ M_\odot$, in agreement with the M/M_b shown in table 3 . However, warm DM faces two problems, one on large scales and one on small scales. On large scales, the question is whether the model can account for the observed network of filaments and voids seen in the universe. Detailed N-body simulations ($N \sim 10^6$) may be needed to answer this. The same difficulty comes in the case of cold DM also, as we shall see later. On small scales, dwarf galaxies pose a problem to the warm DM picture. The phase constraint here is satisfied unlike in the hot DM case, since these particles are of larger masses ($m_w \sim 1\ KeV$), but the problem here is about the formation of dwarf galaxies. Warm DM damps out fluctuations below M_{Jw} ($\sim 10^{12}\ M_\odot$) and dwarf galaxies with $M \sim 10^7 M_\odot$ can only form via fragmentation, following the collapse of a protogalaxy. The problem here is that dwarf galaxies, having small escape velocities, $\sim 10\ Km \cdot sec^{-1}$, can capture only a small fraction of the warm DM particles, whose typical velocity dispersion must be $\sim 100\ Km \cdot sec^{-1}$, typical of ordinary spiral galaxies. Thus, we expect M/M_{lum} for dwarf galaxies to be much smaller than for galaxies, but this is not so, as seen from the fig. 19 .

The detailed theory needed for fragmentation process is applicable here too, since some process of fragmentation would be needed to form small galaxies. Though some of the problems faced with hot DM are resolved here, there are difficulties in the warm DM scenario too. And of course, right now there is no suitable candidate for warm DM.

3.4 GALAXY FORMATION WITH COLD DM

There are some collisionless particles which decouple when they are non-relativistic. These particles are either more massive than the warm DM particles ($m_c > 1\ KeV$) or are "cold" in the sense of having very little velocity dispersion at all times. An example of the former is the photino mentioned earlier with $m_{\tilde{\gamma}} \sim 2$ GeV. An example of a " cold" particle having little velocity dispersion is the axion, a spin zero pseudo-Goldstone boson which has been proposed to explain the absence of CP violation in strong interactions within the context of quantum chromodynamics (QCD) (Peccei and Quinn 1977; Weinberg 1978; Wilczek 1978). The constraints from the

critical density ρ_c (Preskill et.al. 1983) and the longevity of helium burning stars (Fukugita et.al. 1982) put limits on the mass of the axion m_a , as

$$10^{-5}\ \text{eV} \lesssim m_a < 10^{-1}\ \text{eV}$$

For $m_a \approx 10^{-5}$ eV , the axions today would be gravitationally dominant. A third cold DM candidate is black holes of mass $10^{-16}\, M_\odot \lesssim M_{BH} \lesssim 10^{6}\, M_\odot$ the lower limit is implied by the non-observation of γ -rays from black hole decay by Hawking radiation and the upper limit is required to avoid disruption of galactic disks and star clusters(Carr 1978; Freece 1983). Another exotic cold DM candidate is the quark nugget (Witten 1984). Thereis no shortage of cold DM candidates, though till now none have been proved to exist in nature.

THE FLUCTUATION SPECTRUM FOR COLD DM

The growth of cold DM fluctuations was first calculated numerically by Peebles(1982) who included cold DM , photons, baryons, and electrons and ignored neutrinos. He calculated the fluctuation spectra and gave it the analytic form(Peebles 1982)

$$|\delta_k|^2 = K^n \left[1 + \alpha K + \beta K^2\right]^{-2} \qquad (3.31)$$

where $\alpha = 10.7$ MPC ; $\beta = 8.4$ MPC^2

Blumenthal and Primack (1983,1984) extended these numerical calculations to include three massless neutrino species and found similar results as Peebles.

It is convenient to represent the cold DM spectra in another form, $\frac{\delta M}{M}$, which represents the rms mass fluctuation within a randomly placed sphere of radius R (Peebles 1982). Peebles (1984) gives this in terms of $\xi(r)$, the two-point correlation function

$$\left(\frac{\delta M}{M}\right)^2 = \int_{\mathcal{V}} \xi(r)\ \frac{d^2 r}{r^2}$$

Fig. 15 shows the results for $\frac{\delta M}{M}$, normalized in such a way that

$$\frac{\delta M}{M} = 1 \qquad \text{at} \qquad R = h^{-1}\ \text{MPC}$$

This normalization agrees with the rms fluctuation $\frac{\delta N}{N}$ in the counts of bright galaxies at $R = 8\, h^{-1}$ MPC (Peebles 1980; Davis and Peebles 1983). We see from the figure that at $R < 0.1$ MPC , $\frac{\delta M}{M}$ varies slowly as $|\log R|^{\frac{1}{2}}$.

Figures 15 16

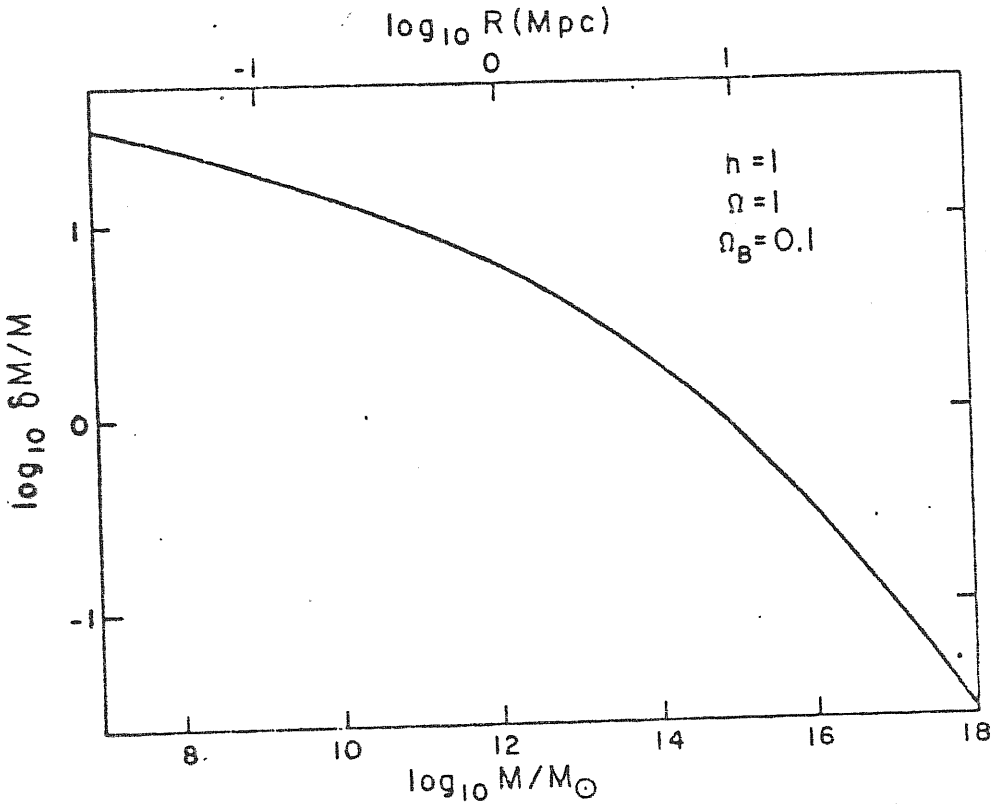

Figure 4. The logarithm of the r.m.s. mass fluctuations ($\log_{10}\delta M/M$) within a randomly placed sphere of radius R in a cold DM universe. The curve is normalized at R = 8 Mpc and assumes an initial Zeldovich (n = 1) fluctuation spectrum.

At large R, $\frac{\delta M}{M} \propto R^{-2}$, which is the primordial spectrum

At $1 \leq R \leq 30$ MPC, $\frac{\delta M}{M}$ varies roughly as $R^{-1.25}$

This applies even in the non-linear regime $\frac{\delta M}{M} >> 1$ at small R.

Fluctuations having masses $M < M_{eq}$ cross the horizon when the universe is still radiation dominated($z > z_{eq}$). After such fluctuations cross the horizon, the neutrino components of the perturbations dissipate by free-st reaming , and the photon and charged particle perturbations oscillate as an acoustic wave, whose amplitude is ultimately damped by photon diffusion(Silk damping). As a result, the growth of cold DM fluctuations δ_c decreases and consequently δ_c begins to grow very slowly until the universe becomes cold DM dominated at z_{eq} after which δ_c grow according to the usual law

$$\left(\frac{\delta \rho}{\rho}\right)_c \equiv \delta_c \propto R = (1+z)^{-1} \qquad (3.32)$$

until $z \approx \Omega^{-1}$. This inhibition of the growth of δ_c , for fluctuation which enter the horizon at $z > z_{eq}$ before the matter dominated era is called "stagspansion"(Primack and Blumenthal 1983).

Since fluctuations of $M < M_{eq}$ grow little during stagspansion and since fluctuations on all scales grow at essentially the same rate after the universe becomes matter dominated,an initial $n = 1$ Zeldovich spectrum evolves to a much flatter spectrum for $M < M_{eq}$. See Fig. 16 . Shown in the figure are also fluctuation spectra for hot DM case and white noise fluctuations ($n = 0$) in an isothermal scenario. The next figure(17) gives the power spectra for all three DM's, hot, warm and cold.

GALAXY FORMATION WITH COLD DM

Though before recombination the baryon fluctuations ($\delta_b \equiv \frac{\delta \rho_b}{\rho_b}$) do not grow and are damped for $M < M_{Silk}$, after recombination the baryons fall into the cold DM perturbations and $\delta_b = \delta_c$ (Doroshkevich et.al. 1980). This occurs when the baryonic fluctuation mass exceeds the baryonic Jeans mass $M_{J,b}$

$$M_b > M_{J,b} \sim 10^6 (\Omega h^2)^{-1/2} \left(\frac{T_b}{T_\gamma}\right)^{3/2} M_\odot \qquad (3.33)$$

where T_b is the temperature of the baryon gas and T_γ is the photon temperature. On scales smaller than this, the pressure of the baryonic gas prevents growth from developing δ_b to be the same as δ_c .

When the fluctuation becomes $\frac{\delta M}{M} \sim 1$ for any mass scale M , non-linear

FIGURE 17

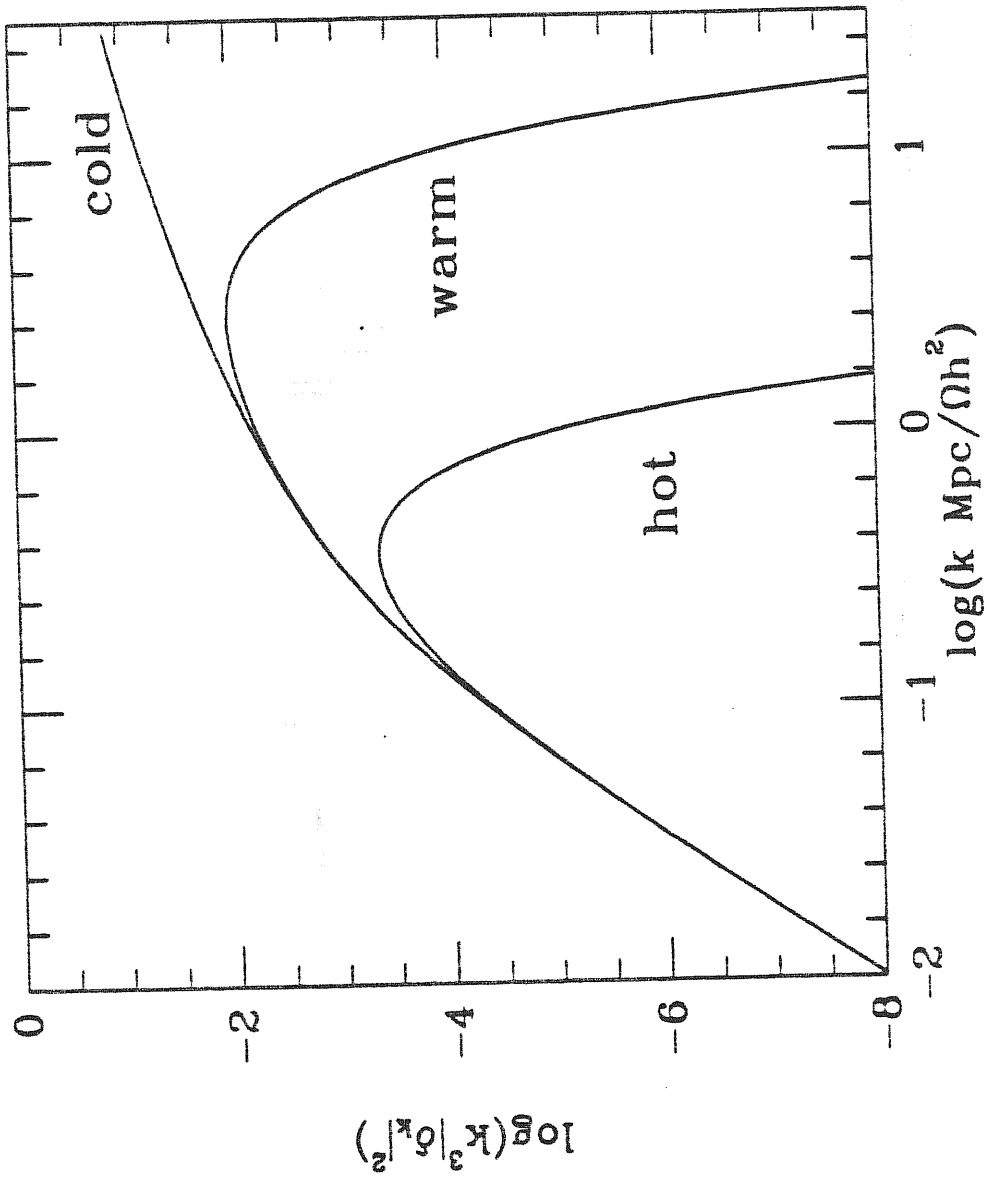

Figure 1.

FIGURE 17

gravitational effects become important. Then the fluctuation separates from the Hubble expansion, reaches a maximum radius and begins to contract. During this contraction, violent relaxation due to the rapidly varying gravitational field converts enough potential energy into kinetic energy for the virial relation

$$\langle PE \rangle = -2\langle KE \rangle$$

to be satisfied(Sargent et.al. 1981; Gott 1977). After virialization, the mean density within a fluctuation is roughly eight times the density corresponding to the maximum radius of expansion(Peebles 1980).

Fig. 16 shows that the cold DM fluctuation spectrum is a decreasing function of M; smaller mass scales become non-linear and collapse first at earlier times than large mass fluctuations. Although small mass fluctuations are the first to go non-linear, we know that pressure effects prevent baryons from falling into such cold DM fluctuations if $M < M_{J,b}$. More importantly,even for $M > M_{J,b}$, the baryons are not able to contract further unless they cool by emitting radiation. Without such mass sagregation between baryons and cold DM, the resulting structures will be disrupted by virialization as fluctuations that contain them go non-linear (White and Rees 1978).

Galaxy formation here proceeds according to the hierarchical scenario, since small scale structures form first. Then these cluster gravitationally to form larger structures. This hierarchical clustering of smaller systems into larger bound systems begins at the baryon Jeans mass $M_{J,b}$, and continues until the present time. It is helpful to visualize the clustering process by means of a diagram that follows the gradual evolution in the properties of collapsed remnants as clustering evolves. This is shown in the figure(17), where the baryonic number density n_b is plotted versus virial temperature T for spherically symmetric protocondensations resulting from $n=1$ Zeldovich spectrumof cold DM fluctuations. The curves in the figure assume that the protocondensations have already virialized but that baryons have not yet cooled and condensed. The curves labeled 1σ assume that for each mass scale, $\frac{\delta M}{M}$ has the appropriate normalized rms value; 2σ corresponds to fluctuations $\frac{\delta M}{M}$ twice as great and so on. Mass labels on the diagonal lines are total values and include DM. The clustering process executes a locus in the (n_b, T) plane, the shape of which is controlled by the form of the fluctuation spectrum. The heavy curve in the figureis the locus corresponding to an average perturbation at amplitude $\langle \frac{\delta M}{M} \rangle$ of 1σ. Also shown in the figure are the present positions of clusters and groups of galaxies, including dwarf spheroidals. It is seen in the figure that the different types of galaxies (the Hubble sequence),

FIGURE 18

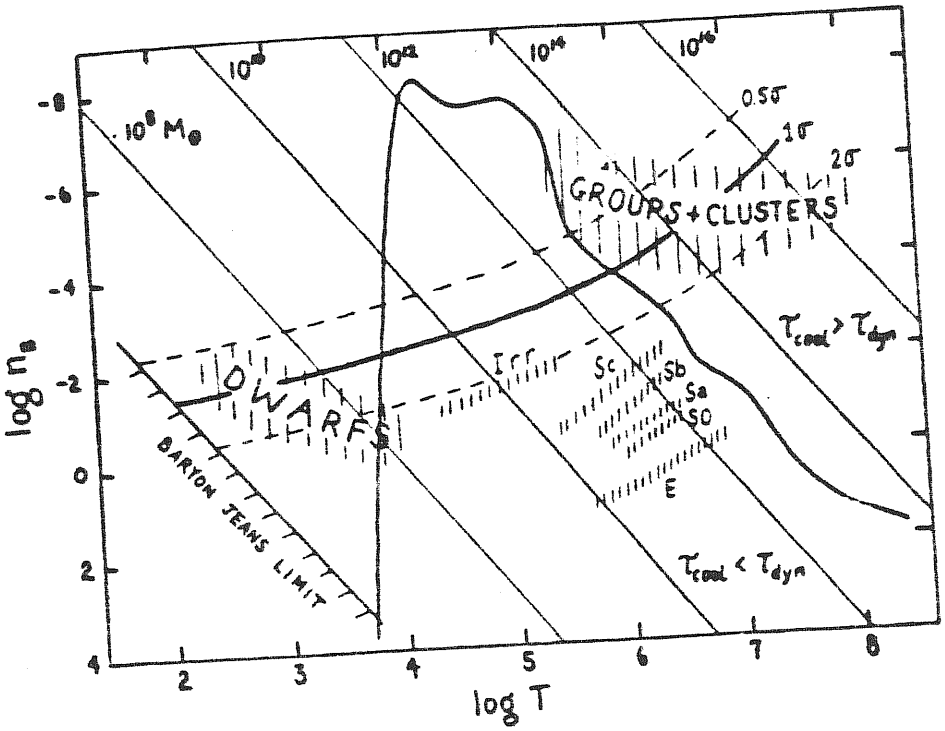

Fig. 2 - The clustering locus in the (n_B,T) plane for the cold-dark-matter DFS of Fig. 1. Heavy line corresponds to 1σ perturbations ($^{\delta}M/M = \langle ^{\delta}M/M \rangle$). Dashed lines show equilibria of 0.5σ and 2σ perturbations. The cooling boundary corresponds to gas with solar composition. Galaxies are plotted according to Hubble type: E = elliptical, SO - Sc = spiral, Irr = irregular. For discussion, see text.

are all spread out.

The choice of (η_B , T) coordinates allows us to identify those structures in which dissipation is important. A good criterion for dissipation (Rees and Ostriker 1977) is to compare the gas-cooling timescale, t_{cool} , to the collapse timescale,

$$t_{dyn} \equiv R/\dot{R}$$

If $t_{cool} \ll t_{dyn}$, baryonic collapse is not halted by internal pressures and the baryonic component collapses dissipatively. The areas $t_{cool} < t_{dyn}$ and $t_{cool} > t_{dyn}$ are shown in the figure.

The figure shows that dissipation is important for galaxies(they lie in the region $t_{cool} < t_{dyn}$). All medium and large-sized galaxies lie in this region. Groups and clusters of galaxies lie in the region $t_{cool} > t_{dyn}$, where cooling is unimportant (Faber 1982; Silk 1982). An important feature in the figure is the marked separation by a factor $\sim 10^3$ in the baryonic density between galaxies on one hand and groups and clusters on the other. This separation can be taken as a strong evidence for dissipation on the scale of galaxies but not in clusters . This gap would disappear if total rather than baryonic density had been plotted. Then galaxies would move to lower densities by a factor ~ 100 as the dark halos are more diffuse than the luminous portions by about this factor, and groups and clusters would move to higher densities by a factor ~ 10 . The apparent gap would then vanish and the clustering process would exhibit an unbroken continuum on all mass scales, as it should in a dissipationless hierarchical clustering.

The position, width and shape of the cold DM clustering locus seems a fair match to the real structures in the universe from $10^6 - 10^{15} M_\odot$. The figure also suggests naively that there is an upper bound for galactic masses of $M \leq 10^{12} M_\odot$, where the baryonic cooling time begins to exceed the dynamical time. For the smallest galaxies , collisional excitation of atomic hydrogen provides a lower limit $M \geq 10^8 M_\odot$, corresponding to virialized baryonic temperature $T_b \geq 10^4 K$. This range $10^8 M_\odot \leq M_{gal} \leq 10^{12} M_\odot$, encompasses virtually all mass that is observed to comprise galaxies. For protogalaxies in this mass range, the velocity dispersion of the baryons will initially remain constant($T \approx const$) as they condense within a gravitational potential of the virialized, presumably isothermal, DM halo.

The collapse of fluctuations with masses $M > 10^{13} M_\odot$ leads to clusters of galaxies in this picture. In this model, there is a natural mass scale(Blumenthal et.al. 1984)

$$M_{J,b} \sim M_{gal,b} \left(T_{virial} / 10^4 K \right)^2 \sim 10^6 M_\odot \qquad (3.34)$$

where $M_{Gal,b}$ is the baryonic mass within a galaxy; $M_{J,b}$ is the Jeans mass of a cloud at 10^4 K in pressure balance with protogalactic gas at the virial temperature. During the dissipation phase of galaxy formation, the gas might be likely to have a two-phase structure with a hot phase at T_{virial} and a cool phase at $\sim 10^4$ K, in which case subcondensations of mass $M_{J,b}$ would be expected with density constant $\approx T_{virial}/10^4$ K. These can be identified with protoglobular clusters. More about this will be given in the next chapter, where we shall discuss the formation of these structures in detail and discuss their role in explaining the formation of structure in the universe.

PROBLEMS WITH COLD DM

Formations of galaxies with cold DM dominating the universe,is an attractive scenario but it has some difficulties which are yet to be solved. Dwarf galaxies with heavy DM halos are less of a problem here but there is the problem of sufficient cooling of baryons and to avoid disruption. The Hubble type versus environment correlation cannot be answered as naturally as in the hot DM case, since it is inherently plausible there that events during cluster collapse might affect the fragmentation process within a cluster. In the hierarchical scenario, galaxies form before clusters without anyforeknowledge of their environment. However work is being done in this direction(Blumenthal et. al. 1984).Peebles(1984) examined statistical correlations between local density peaks and surrounding density enhancements in the cold DM picture and found dense galaxies to lie preferentially in dense clusters. Ellipticals are found in denser regions and irregulars and spirals are found in sparse regions. The figure (18) shows that ellipticals are denser than spirals or irregulars and Peebles' suggestion seems to be verified. However, Peebles strictly refers to the density and distribution of DM whereas the density in the figure(18) refers to baryons. There is a need to link baryonic density of galaxies to the densities of their dark halos in this picture.

A second problem involves the masses of galaxies. In the cold DM picture, these are determined by the rate at which the clustering proceeds relative to the rate at which the baryonic collisional cross-sections of galaxies shrink via dissipation. A complete theory for galaxy masses thus depends on detailed understanding of the dissipation processes, which is still not clearly known(Faber 1984) .

The most serious challenge for cold DM arises on very large scales, where galaxies are observed to form filamentary superclusters with large voids between them (Oort 1983). Numerical simulation of clustering do seem to develop sheets and

filaments(Melott et.al.1983), but poses some problems matching with the real universe.

In order to preserve the attractive features of hot DM universe(large scale structures) and cold DM (small scales), it is worth considering a scenario where the universe is dominated by two kinds of particles, a hot DM particle and a cold DM particle. Work on hot DM particles (neutrinos $m_\nu \sim 30$ eV) and warm DM particles (photinos ~ 1 KeV) together present in the universe has been done by Valdernini et. al. (1983, 1984).

CHAPTER FOUR
THE GLOBULAR CLUSTERS

Globular clusters are the oldest systems in our galaxy. Because of their great age, the study of the formation of globular clusters is intimatly involved with cosmology. The formation of these cluster systems with masses $\sim 10^6 M_\odot$ inside galaxies,is still an unsolved problem. It was generally believed that the globular clusters in our galaxies formed through contraction after the galaxy has come into existence. But, because the Jeans mass just after recombination is so near the observed mass of globular clusters, many investigators argued that the growing condensations at the epoch of recombination should be associated with the formation of globular clusters.

Impressed by the apparent uniformity of globular cluster luminosities, both throughout our galaxy and in other galaxies, Peebles and Dicke(1968) proposed that globular clusters originated as gravitationally bound gas clouds before the galaxies have formed. In their model, the first bound systems to have formed in the expanding universe were gas clouds with mass and shape quite similar to the globular cluster systems. Prior to the recombination epoch, radiation drag on the matter prevents the growth of irregularities and at recombination the Jeans mass is $\sim 10^5 M_\odot$. Since this is of the order of a globular cluster mass, Peebles and Dicke proposed that globular clusters came into existence before galaxies did. They also suggested that the formation of larger systems in the universe takes place by the merging of these protoglobular clusters. Van den Berg (1975) has pointed out, however, that globular clusters do seem to differ systematically in certain traits from one galaxy to another, which may argue for a postgalaxy formation for the globular clusters. He pointed out that the Peebles and Dicke scenario leaves a number of observational questions unanswered. Maybe by studying the various properties exhibited by these systems, we might get an idea about the formation of globular clusters. And, as Peebles and Dicke suggested, if they are really cosmological objects, then from the studies of globular clusters, we might have some clues about the formation of structures in the universe, which as we have seen in the last chapter, is still an unsolved problem. Let us consider the formation of these objects in the spirit of the arguments given in the last chapter and see whether the results are consistent with the observed properties of these cluster systems.

DARK MATTER AND GLOBULAR CLUSTERS

In a universe dominated by weakly interacting particles with negligible primeval pressure, the cold DM , assuming adiabatic fluctuations, we find that there exists a characteristic mass scale for baryons

$$M_b \sim 10^6 M_\odot \qquad (4.1)$$

which can be identified with the masses of globular clusters. The power spectrum for the cold DM , P_c (Peebles 1982), is given by the expression (see eqn. 3.31)

$$P_c \equiv |\delta_k|^2 \propto K (1 + \alpha K + \beta K^2)^2 \qquad (4.2)$$

where $\alpha = 10.7$ MPC , $\beta = 8.4$ MPC^2
and K is the comoving wave number($K = \frac{2\pi R(t)}{\lambda}$) expressed in units of radians per MPC at the present epoch. At small K , $P_c \propto K$, which is the initial primeval Zeldovich spectrum with $n = 1$. At short wavelengths the spectrum is suppressed by radiation pressure, so $P_c \propto K^{-3}$ at large K . The first generation of objects form at $z \sim 100$ in this scenario. At $z \sim 100$ hydrogen decoupled from the radiation and thus relaxed to the same distribution as the cold DM longward of the hydrogen Jeans length. The gas pressure suppresses density fluctuations on smaller scales. The resulting spectrum for the hydrogen was calculated by Peebles (1982) and is given by the expression

$$P_H = \frac{P_c}{(1 + \gamma K^2)^2} \quad , \quad \gamma = 2.6 \times 10^{-6} \text{ MPC}^2 \qquad (4.3)$$

At comoving wavelengths ~ 10 KPC to ~ 1 MPC , $P_H \propto K^{-3}$, so the contribution to the variance of $\frac{\delta \rho}{\rho}$ per octave of wavelength is constant. The spectrum is normalized by fitting to the observed large scale fluctuation in galaxy counts (see fig. 16) as shown before.

The sizes of the smallest structures are fixed by the short wavelength cutoff of the $P_H \propto K^{-3}$ spectrum. For the hydrogen distribution this cutoff is fixed by the Jeans length and one finds that the hydrogen mass in one of these gas clouds is (Peebles 1984)

$$M_b \sim 4 \times 10^6 M_\odot \qquad (4.4)$$

As noted by Peebles and Dicke, this is coincident to the mass of a globular cluster. The clouds also tend to appear in associations, an unusually dense cloud tending to be surrounded by other dense clouds. The characteristic mass of an association is fixed by the break in the spectrum $P_c(k)$. This mass might be associated with a galaxy mass (Peebles 1982). Thus a universe dominated by cold DM yields two characteristic scales, one of which might be identified with galaxies, and the other with globular clusters.

The quantitative analysis of the hydrogen mass distribution implied by the spectrum $P_H(k)$ in the model is given by considering a fractional mass excess Δ within a distance r of a peak of the baryon mass density $\delta\rho_b$ (Peebles 1984)

$$\Delta = \int_r d \quad \delta\rho_b / (\langle\rho\rangle V) \qquad (4.5)$$

If $\delta\rho_b$ is a random gaussian process the probability distribution of Δ from the spectrum $P_H(k)$ can be derived.

Fig. 19 shows the behaviour of Δ around a two standard deviation extremum of $\delta\rho_b$ The central curve is the mean value of Δ . The top and bottom curves are shifted from the mean by the rms fluctuation of Δ around the mean . The horizontal axis is the comoving distance r from the extremum of $\delta\rho_b$. The top scale is the mean baryon mass M_b within a sphere of radius r .

One sees from the figure that there is a considerable spread in the mass excess found around a peak in the baryon mass density. One also sees that the denser gas clouds reach a density contrast $\Delta \sim 1$ and start to break away from the general expansion at a redshift $z \sim 60$. This is the first generation of hydrogen objects. Around such a dense spot there is a net mass excess ($\Delta > 0$) that tends to extend to $M_b \sim 10^{10} M_\odot$, but with a considerable scatter.

A fluctuation (upward) 1σ in Δ produces a region with baryon mass $M_b \sim 10^{11} M_\odot$. This tends to form a bound system by $z \sim 10$. A fluctuation less than 1σ gives a mass $\sim 10^8 M_\odot$. Thus at $z \sim 10$ the objects just forming would have baryon masses roughly in the range observed for galaxies.

At redshift $z \sim 50$, the most prominent (3σ)peaks of the hydrogen distribution develop into a first generation of gas clouds with radii ~ 1 KPC and baryon masses $M_b \sim 10^6 M_\odot$. The temperature of the hydrogen is $T \sim 100^\circ K$. This is close to the background temperature because the residual ionization is high enough to allow a

FIGURE 19

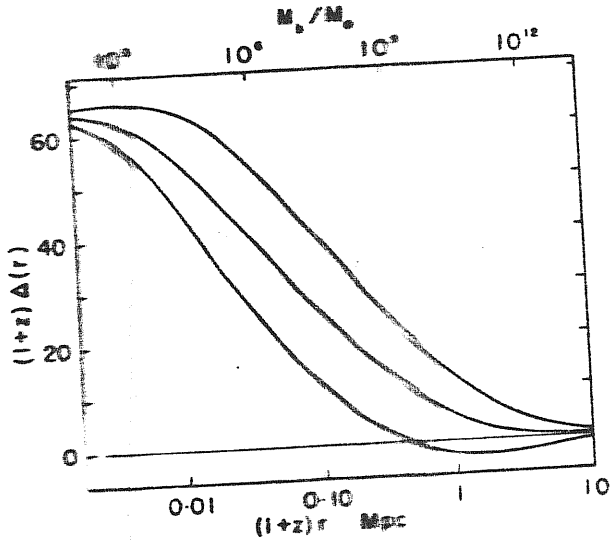

FIG. 3.—The fractional mass excess Δ within distance r of a spot where the baryon density contrast is twice the mean value. The middle curve is the mean value of Δ (eq. [24]). The top and bottom curves are the rms fluctuation around the mean. The curves are normalized by eq. (9).

appreciable heat transfer from radiation to matter(Peebles 1968). This means that once the gas cloud stops expanding and is supported by gas pressure, it can lose energy, shrink and heat it up. When the gas temperature reaches $\sim 10^4 K$, the matter gets collisionally ionised, the cloud radiates more and the central part of the clouds tend to collapse in a free fall manner. The final structure would be a radius of the order 20 to 30 Pc , which is not unreasonable for a globular cluster(Harris and Racine 1979).

GLOBULAR CLUSTERS WITH MASSIVE HALOS

In the above scenario, the first hydrogen forms at $z \sim 50-100$ as gas clouds with size ~ 1 KPC . Since the initial density fluctuations were supposed to be adiabatic the cloud would be formed with comparable concentrations of hydrogen and DM the mass density of the DM being ~ 30 times larger, the net mass of the cloud is around $\sim 10^7 M_\odot$. Since the DM is weakly interacting it is left behind when the hydrogen cloud coctracts. This makes the final central density of the star cluster substantially larger than the DM density. This is rather desirable because the observed mass -to-light ratios in the coresofglobular clusters are approximately unity. But this picture suggests that a globular cluster,like some galaxies,is born with an extended halo of DM . There is no observational evidence that globular clusters have massive halos but Peebles (1984) pointed out that there is not much direct contrary evidence either.In fact, he suggested that if globular clusters do have DM halos they might help to account for some of the systematics of the globular cluster properties.

TESTS FOR MASSIVE HALOS IN GLOBULAR CLUSTERS

Dwarf spheroidal galaxies are found to be dominated by DM halos(Aaronson 1983; Faber and Lin 1983). It is not unreasonable to extend this argument to globular clusters, which are only one order of magnitude in mass smaller than the dwarf galaxies but similar to them in most of their other properties. Since the baryonic mass gets concentrated to the central region of the globular clusters and the DM forms a halo around them, we can check if the mass-to-light ratios in these systems increases with radius as it does in a spiral galaxy. Another test is to see whether the line-of-sight velocity dispersion for these objects increases with increasing radius. The observational possibilities to check for the presence of a dark DM halo in globular clusters will be discussed later. However it is interesting to note that a massive halo produces an apparent tidal cutoff in

a cluster, similar to the tidal cutoff observed in these systems. In this picture the density of a cluster varies as

$$\rho \propto (-\phi/\sigma^2) \qquad (4.6)$$

where ϕ is the gravitational potential and σ is the 1-dimensional velocity dispersion. If ϕ at large radius is dominated by the DM it can sharply cut off ρ. For example suppose the core radius of the dark material is much larger than the size of the cluster so that the DM adds a constant value ρ_x to the netmass density. Then the Emden's isothermal gas sphere equation becomes

$$\frac{1}{z^2}\frac{d}{dz}\left(z^2\frac{d\nu}{dz}\right) = e^{-\nu} + \frac{\rho_x}{\rho_0} \qquad (4.7)$$

where $r = \alpha z$, $\alpha^2 = \frac{\sigma^2}{4\pi G \rho_0}$, $\rho = \rho_0 \exp(-\nu)$

and ρ_0 is the central mass density.

Fig. 20 shows the projected surface density in the model. The top curve is for $\rho_x = 0$. The second curve is for an isothermal gas sphere with a homogenous dark halo with density $\rho_x = 0.2\%$ of the central density. The bottom curve is the ratio of the net mass to the star mass within a sphere of radius r for the second curve. Compare this with the figure 21 which shows the density distribution observed in globular clusters as calculated from their star counts (King 1966). The real clusters are tidally limited by the parent galaxy. The limiting tidal radius of the cluster is given by the formula

$$r_t = R_p \left[\frac{m}{(3+e)M_g}\right]^{1/3} \qquad (4.8)$$

where R_p is the perigalacticon distance of the cluster, m and M_g are the masses of the cluster and the galaxy respectively and e is the eccentricity of the cluster's orbit.

The density distribution seen in the figure(21) was fitted by a formula

$$f = f_1\left(\frac{1}{r} - \frac{1}{r_t}\right)^2 \qquad (4.9)$$

where f is the surface density, f_1 is a constant and r is the radius of the cluster. Also, an empirical formula was found by King(1962) which represents the

FIGURE 20

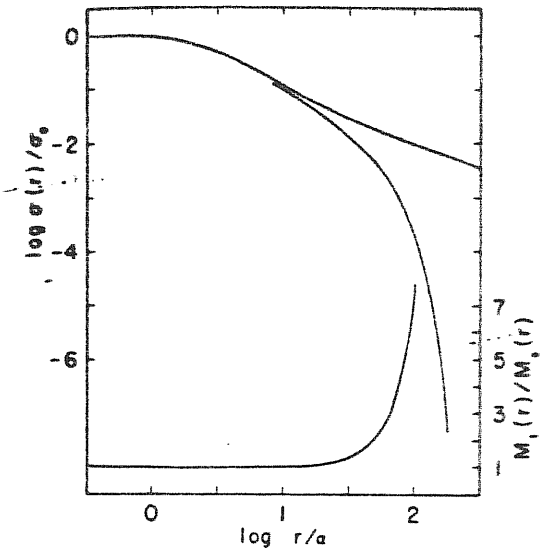

FIG. 4.—A globular cluster model. The top two curves show projected surface star densities. The upper curve is the classical Emden isothermal gas sphere, the second curve is an isothermal gas sphere with a homogeneous dark halo with density 0.2% of the central star density. The bottom curve is the ratio of the net mass to the star mass within a sphere of radius r for this second model.

FIGURE 21

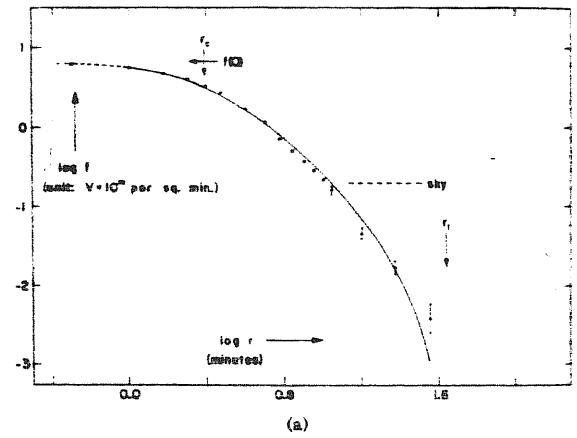

(a)

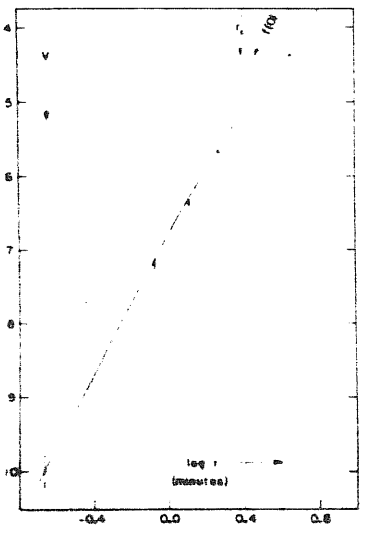

(b)

FIG. 10. Test of Eq. (14) in ω Centauri (Gascoigne and Burr): (a) outer parts, (b) central region.

density from centre to edge in globular clusters. This is given as

$$f = k\left[\frac{1}{[1+(r/r_c)^2]^{1/2}} - \frac{1}{[1+(r_t/r_c)^2]^{1/2}}\right] \qquad (4.10)$$

where k is a constant and r_c is a scale, called the core radius. King found that this law agrees quite satisfactorily with the observational data. He found that the density distributions in all the globular clusters can be represented by this law. The shape of the density curve calculated for a globular cluster with dark halo is similar to that of a King model. As expected the DM becomes dominant at the effective " tidal" cutoff. However, this dark halo model is not consistent with observations in the case of Omega Centauri. Seitzer (1983) has found that the line-of-sight velocity dispersion decreases with increasing radii at the rate expected for King's model with no dark halo. Gunn and Griffin (1979) found evidence of decreasing line-of-sight net dispersion with increasing radius in M3 and they also obtained a satisfactory fit to the star distribution and motions using a truncated model with an anisotropic velocity distribution and no DM. However, it is worth emphasizing that the anisotropy of the star orbits introduces an uncertainity into the measurement of the mass distribution (Peebles 1984). The equation of equilibrium for a star distribution is given by

$$\frac{d}{dr}\left(\rho v_r^2\right) + \frac{2\rho}{r}\left(v_r^2 - v_a^2\right) = -g\rho \qquad (4.11)$$

where g is the gravitational acceleration , $\rho(r)$ is the mean star mass density, v_r , v_a are the radial and azimuthal velocity dispersions respectively. If the dilute halo of a star cluster were populated by relaxation in the core, we would expect $v_r \gg v_a$. If v_r were roughly constant, then because $\rho(r)$ is decreasing appreciably more rapidly than r^{-2} in the outer envelope, eqn. (4.11) would say that the total mass density varies as $\rho_x \propto r^{-2}$, indicating the presence of DM. The best evidence on the behaviour of v_r comes from Cudworth's (1979) studies of relative peculiar star motions within globular clusters. Cudworth found that v_r in M3 , is roughly constant to $r \sim 0.25\, r_t$, a radius that contains 90% of the stars. However, this constant v_r cannot be taken as the evidence for DM in globular clusters because the flat shape of observed might be a result of measuring errors at large r . However, this is an interesting test to check whether globular clusters have DM.

A massive DM halo in globular clusters means that their net mass-to-light value is larger. Right now, there is no direct observational evidence for this. But Innannen et. al. (1983) found that a discrepancy in their calculations disappears if they use a higher m/l , than the one they have taken. Innannen et.al. investigated shapes of globular cluster orbits in our galaxy, using the tidal radii of the clusters as probes of the galactic gravitational field at their perigalactic points.

The observational problem of measuring the tidal radius of a real cluster employs the run of projected star density with radius from the cluster centre. Typically, the cluster contribution to the projected density of stars is overwhelmed by random fluctuations in the background density before even half of the apparent tidal radius can be reached(King et.al. 1968). But within this relatively small region of the cluster, tidal distortion of the cluster shape is small/ For this reason, the observed projected density profile of a cluster is then invariably fitted with a spherical model, as a means,extrapolating the observed profile from the inner parts of the cluster out to a radius at which the density vanishes according to the cluster model.Thus , the " measured" tidal radii may not always be without error.

Innannen et.al. assumed a spherically symmetric mass distribution model for the galaxy with the mass $M(R)$ increasing linearly with R

$$M(R) \propto R \qquad (4.12)$$

in their calculation. The theoretical expression for the tidal radii for the globular clusters in our galaxy calculated by them was

$$r_t = \frac{2}{3} R_p \left[1 - \ln (R_p/A) \right]^{-1/3} \left[\frac{m}{2M_g} \right]^{1/3} \qquad (4.13)$$

where R_p is the perigalactic distance of the globular cluster, A is the semi-major axis of the orbit. m , M_g are the masses of the globular cluster and the galaxy respectively. For a point mass galaxy, this expression reduces to

$$r_t = \frac{2}{3} R_p \left[\frac{m}{(3+e) M_g} \right]^{1/3} \quad ; \quad e = (1 - R_p/A) \qquad (4.14)$$

which is similar to the one derived by King (see eqn.4.8) except for the factor $\frac{2}{3}$. This difference arises from the elongation of the limiting tidal surface along the line between the cluster centre and the galactic centre (Keenan 1981). King's r_t value actually refers to the distance along this axis from the cluster centre to the analogue of the inner lagrangian point in the elliptic restricted

three-body problem for a point-mass galaxy.

In order to relate the theoretical radii of eqn.(4.13) to the actual observational data, Innannen et.al. found that the value of r_t needed was

$$r_t\,(\mathrm{KPc}) = \frac{r_o\, r_t'}{3438} \qquad (4.15)$$

where r_o is the heliocentric distance of the cluster in KPC' and r_t' is its observed angular tidal radius in arc minutes.

The cluster mass 'm' they had, was obtained from its visual mass-to-light ratio, m/ℓ, through

$$m = \left(\frac{m}{\ell}\right)_V \ell_V = \left(\frac{m}{\ell_V}\right) 10^{0.4\,(M_V(\odot) - M_V)} \qquad (4.16)$$

where M_V is the visual integrated absolute magnitude of the cluster. Using the Harris and Racine data (1979) they found ,

$$(m/\ell)_V = 1.7 \pm 0.2 \qquad (4.17)$$

This $(m/\ell)_V$ was assumed to be the same on average for clusters everywhere in the galactic halo. Real cluster-to-cluster differences might exist but the mean value might be approximately given by (4.17). The cluster perigalactic distances R_p were determined by them as follows: using eqns.(4.12), (4.13) and (4.14) , they found that the cluster mean density can be written as

$$\bar{\rho}_c \equiv \frac{3m}{4\pi r_t^3} = \frac{81}{16\pi}\left[1 - \ln\left(R_p/A\right)\right]\frac{1}{R_p^2} \qquad (4.18)$$

This $\bar{\rho}_c$ can be written directly in terms of observational quantities as

$$\bar{\rho}_c = \frac{3}{4\pi}\left(\frac{m}{\ell}\right)_V 10^{0.4[M_V(\odot) - M_V]}\left(\frac{r_o\, r_t'}{3438}\right)^{-3} \qquad (4.19)$$

But eqn. 4.18 has two unknown quantities A and R_p . Fortunately, for objects orbiting in logarithmic potential the time-averaged mean of $\ln\left[R_p/R(t)\right]$ isjust given by

$$\left\langle 1 - \ln\left[R_p/R(t)\right]\right\rangle = 1 - \ln\left(R_p/A\right) \qquad (4.20)$$

Thus, by substituting the presently observed galactocentric distance, R, of each cluster for A in eqn.(4.20), and multiplying both sides of this equation by R^2, one gets a transcendental equation for an unbiased estimate of $\langle R_p/R \rangle$ in terms of $\bar{\rho}_c R^2$.

Using this, Innannen et.al. derived the perigalactic distances for 66 clusters in our galaxy as functions of their present galactocentric distances. A histogram of $\langle R_p/R \rangle$ distribution is shown in the fig.(22). But the theoretical distribution curve used in the figure differs from the distribution of perigalactic radii derived from the observed cluster radii. The perigalactic distance for all clusters combined from observations is given by

$$\langle \log (R_p/R) \rangle_{obs} = -0.103 \pm 0.023$$

The theoretical value derived by Innannen et. al. was

$$\langle \log (R_p/R) \rangle_{Th} = -0.031 \pm 0.028$$

To remove this discrepancy, Innannen et.al. found that the mass-to-light ratios have to be increased by a factor 2 to 3 times more than the one they used in the calculation (eqn.(4.17)). Peebles (1984) suggests that this can be considered as evidence for dark halos in globular clusters.

If there is a dark halo in globular clusters, it might act as a trap for high velocity stars, since the escape velocity of the cluster is then larger. The high velocity stars found around Omega Centauri (Seitzer 1983) may be explained by this. But as pointed out before Omega Centauri shows no evidence for a halo. In fact, it gives evidence against a dark halo because it shows a decreasing velocity dispersion with increasing radius. Maybe detailed studies on Omega Centauri are needed to resolve this problem.

Moreover, if a cluster has a dark halo whose radial cutoff in star density is due to the halo rather than a tidal effect, evaporation of stars would be strongly suppressed and the core collapse might be prevented. The core collapse is a maior problem in globular clusters. Numerical studies have indicated core collapse to be common in globular clusters but none have been observed.

FIGURE 22

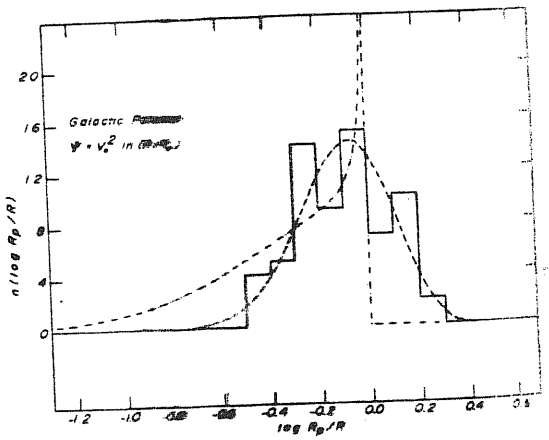

FIG. 2. The distribution of fractional perigalactic distances, R_p/R, for the same potential as Fig. 1. The histogram plotted with a solid line reproduces the distribution inferred observationally in Fig. 1. The dashed line corresponds to a Gaussian distribution in $\log \bar{\rho}_c R^3$, with the observed standard deviation in that parameter, and the dash-dotted line to the theoretically expected distribution for a strictly normal nonrotating cluster system, with velocity dispersion $\sigma = v_c/\sqrt{3}$.

The core collapse problem would not arise for globular clusters formed with a dark halo.

If globular clusters are born with massive halos, it might play an interesting role in the origin of the heavy elements in the cluster stars. In the present picture, protoglobular clusters are the first generation, so the heavy elements must originate by processing stars within the cloud. The dark halo would increase the binding energy of the gas cloud, making it more likely to survive the supernovae from early star generations. Furthermore, the binding energy is highest in the earliest gas clouds and these tend to appear in associations in the densest parts of the most massive protogalaxies. It therefore seems reasonable to speculate that the final heavy element abundances in the cluster is statistically correlated with the density of the halo, because the higher the binding energy the greater the probability that the cloud can survive one or more supernovae and so accumulate heavy elements. Maybe, this can account for the correlation of heavy element abundance with galactocentric distance observed for globular clusters (Harris and Canturna 1979).

Another important point that can be solved in this picture is the high abundance of globular clusters found in elliptical galaxies. Harris and Racine (1979) estimated the total number of globular clusters in a sample of elliptical and spiral galaxies. This total number was derived via the luminosity function for globular clusters, which they find to be fairly uniform from galaxy to galaxy. For most ellipticals, the total number is closely proportional to the integrated luminosity of the galaxy. The spiral galaxies appear to have fewer clusters than do the ellipticals.

Van den Bergh (1982) has also shown that there is a relatively high abundance S of globular clusters per unit spheroidal luminosity in M87 and other first-ranked galaxies. If the formation of elliptical systems in the universe was by merging, then it would be difficult to explain this high S .

Toomre (1977) pointed out that there are at least 11 strongly interacting pairs of galaxies among 4000 NGC galaxies. Adopting a uniform rate of mergers, a merger time-scale of $\sim 5 \times 10^8$ yr. and a Hubble time of 13×10^9 yrs. we get a total of ~ 250 merged galaxies among objects in the NGC. Toomre suggests that if the few mergers we see today are just the statistical drags of a once common process, then the actual number of merger remnants might be actually as high as 750, which is $\sim 19\ \%$ of all NGC galaxies. This value is reasonably close to the value of $14\ \%$

ellipticals found among the Shapley-Ames galaxies (Sandage and Tamann 1981). This approximate numerical coincidence and computer calculations describing collisions between n-body systems, suggest that ellipticals might have been formed by merging of spiral galaxies. We can check this by studying the globular cluster abundance in galaxies.

Most globular clusters are tightly bound objects that will be able to survive the merger of two ancestral galaxies. N-body simulations (Gerhard 1981) have shown that few globular clusters would escape during a merger. Therefore it follows that the specific globular cluster frequency S should be the same in spirals as in elliptical galaxies formed by merging. But this is not what the observations indicate; the frequency S in spiral galaxies is an order of magnitude lower than that in ellipticals. This suggests that elliptical galaxies cannot have formed by mergers of spirals,and galaxies with large S must have been born that way. In the present scenario,that could come about because the most massive protogalaxies would tend to have the greatest initial density contrast and so to have the most durable globular clusters. This scenario for the formation of globular clusters in galaxies is promising and further work has to be done in order to prove or disprove it.

The studies of globular clusters in galaxies give information about the formation of structure in the universe. In a cold DM dominated universe, globular clusters are the first bound objects to form . But these globular clusters are born with a halo of cold DM around them. Right now, there is no strong observational evidence for globular clusters to have massive halos, but as we have seen, if these halos exist, they might actually account for the observed globular cluster systematics. Moreover, if halos are present in globular clusters, it might be an evidence for the existence of cold DM in the universe. A major concern, whether a hierarchical or a pancake model for clustering in the universe is correct, might also be solved from the studies of globular clusters. If globular clusters have formed as suggested, we then have evidence for hierarchical clustering in the universe. This would be an important step forward in our understanding of the formation of structure in the universe.

ACKNOWLEDGEMENTS

I am thankful to my supervisor, Prof. D.W.Sciama, for introducing me to this problem and for his guidance and encouragement during my course of study.

I am grateful to J.Miller, K.Maeda , P.Mann and R.Semenzato for numerous discussions in the course of this work.

I am also specially thankful to Prof.M.Hack for allowing me the use of the facilities of the Trieste Observatory.

I also wish to thank all my colleagues who helped me in the preparation of this dissertation.

REFERENCES

Aaronson, M. (1983).Ap. J. Lett.266, L11.

Aarseth,S.J. et.al. (1979). Ap.J.228,664.

Arnett,W.D. (1978). Ap.J.219,1008.

Audouze,J. (1979). In Physical cosmology, Les Houches Lectures, R.Balian, J.Audouze and D.N.Schramm (Eds.)(North-Holland).

Bahcall,N.A. and Soneira R.M.(1982). Ap.J. Lett.258, L17.

Bardeen,J.M. (1982). Preprint.

Barrow,J.D. and Carr, B.J. (1978). M.N.R.A.S.,181,719.

Blumenthal,G.R. et.al. (1982). Nature 299,37.

Blumenthal,G.R. et.al. (1984). SLAC-PUB-3307.

Bond,J.R. et.al. (1980). Phys.Rev.Lett.45,1980.

Bond,J.R. and Szalay,A.S. (1981). In Proceedings Neutrino '81 (Hawaii), p.59.

Bond,J.R., Szalay,A.S. and Turner,M.S. (1982). Phys.Rev.Lett.48,1636.

Bond,J.R. et.al. (1983). Nature 301,584.

Bond,J.R. and Szalay,A.S. (1983). Ap.J. 274,443.

Burstein, D. et.al. (1982). Ap.J. 253,70.

Cabbibbo,N. et.al. (1981). Phys. Lett. 105B,155.

Carr,B.J. (1975). Ap.J. 201,1.

Carr,B.J. (1978). Comments on Astrophys. 7,161.

Carr,B.J. and Silk,J. (1983). Ap.J. 268,1.

Centrella,J. and Melott,A.L. (1983). Nature 305,196.

Chincarini,G. et.al. (1981). Ap.J.Lett. 249,L47.

Cowsik,R. and McCllelland,J. (1972). Phys.Rev.Lett. 29,669.

Cudworth,K.M. (1979). A.J. 84,1312.

Davis,M. et.al. (1976). Ap.J. 208,13.

Davis,M. et.al. (1980). Ap.J.Lett. 238,L113.

Davis,M. et.al. (1982). Ap.J. 253,423.

Davis,M. and Peebles,P.J.E. (1983). Ap.J. 267,465.

Daum, et.al. (1978). Phys.Lett. 74B,126.

Dekel,A. and Shaham,J. (1979). Ast. and Ap. 74,269.

Dolgov,A.D. and Zeldovich,Y.B. (1981). Rev.Mod.Phys. 53,1.

Doroshkevich,A.G. et.al. (1974). In IAU Symp. No.63,M.S.Longair(Ed.) Reidel,Dodrecht.

Doroshkevich,A.G. et.al. (1980). M.N.R.A.S. 192,321.

Doroshkevich,A.G. et.al. (1981). In Tenth Texas Symposium on Relativistic Astrophysics, R.Ramaty and F.C.Jones(Eds.)(Ann. N.Y.Acad.Sci.,375,p.32)

Efstathiou,G. and Eastwood,J.W. (1981). M.N.R.A.S. 189,203.

Efstathiou,G. et.al. (1983). Preprint.

Faber,S.M. and Gallagher,J.S. (1979). Ann.Rev.Astr.and Ap. 17,135.

Faber,S.M. (1982). In Astrophysical Cosmology, H.A.Bruck, G.V.Coyne and M.S.Longair (Eds.), Pontificia Academia Scientiarium, p.219.

Faber, S.M. and Lin,D.N.C. (1983). Ap.J.Lett. 266,L21.

Faber, S.M. (1984). Preprint.

Fall,S.M. (1979). Rev.Mod.Phys. 51,21.

Freece,K. (1983). Preprint.

Frenk,C.S. et.al. (1983). Ap.J. 271,417.

Fry,J.N. and Peebles,P.J.E. (1978). Ap.J. 221,19.

Fukugita,M. et.al. (1982). Phys.Rev.Lett. 48,1522.

Gerhard,O.E. (1981). M.N.R.A.S. 197,179.

Gershtein,S.S. and Zeldovich,Y.B. (1966). JETP Lett. 4,120.

Goldberg,H (1983). Phys.Rev.Lett. 50,1419.

Gott,J.R. and Rees,M.J. (1975). Ast. and Ap. 45,365.

Gott,J.R. (1977). Ann.Rev.Ast.Ap. 15,235.

Groth,E.J. and Peebles,P.J.E. (1977). Ap.J. 217,385.

Gunn,J.E. and Tremaine,S. (1979). Phys.Rev.Lett. 42,407.

Guth,A. (1982). Phys.Rev.Lett. 49,1110.

Harris,W.E. and Canturna (1979). Ap.J.Lett. 231,L19.

Harris,W.E. and Racine,R. (1979). Ann.Rev.Ast.Ap. 17,241.

Harrison, E.R. (1970). Phys.Rev. D1,2726.

Hawking,S.W. (1983). Preprint.

Hawking,S.W., Gibbons,G.W. and Siklos,S.T.C. (Eds.) The Very Early Universe, Cambridge (1983).

Hegyi,D.J. and Olive, K.A. (1983). Phys.Lett. 126B,28.

Hiyoshi,K. and Kihara,T. (1975). Pub.Astr.Soc.Jpn. 27,333.

Hodge,P.W. (1971). Ann.Rev.Ast.Ap. 9,35.

Innannen,K.A. et.al. (1983). A.J. 88,338.

Kaiser,N. (1983). Ap.J.Lett. 273,L17.

Keenan,D.W. (1981). Ast. and Ap. 95,334.

King,I.R. (1962). A.J. 67,471.

King,I.R. (1966). A.J. 71,64.

King,I.R. et.al. (1968). A.J. 73,456.

Kirschner,R.P. et.al. (1979). A.J. 84,951.

Kirschner,R.P. et.al. (1981). Ap.J. Lett. 248,L57.

Kirstein,T. et.al. (1983). Phys.Rev. Lett. 50,474.

Klypin,A.A. and Shandarin, S.F. (1983). Preprint.

Kwon,H. et.al. (1981). Phys.Rev. D24,1097.

Limber,D.N. (1954). Ap.J. 119,655.

Lin,D.N.C. and Lynden-Bell,D. (1982). M.N.R.A.S. 198,707.

Lin,D.N.C. and Faber,S.M. (1983). Ap.J.Lett. 266,L21.

Lyubimov,V.A. et.al. (1980). Phys.Lett. 94B,266.

Marx,G. and Szalay,A.S. (1972). Proc. Neutrino '72 1:123. Technoinform, Budapest.

Melott,A.L. (1983). M.N.R.A.S. 202,595.

Meszaroes,P. (1974). Astr.and Ap. 37,225.

Olive,K.A. (1981). Nucl.Phys. 190B,483.

Olive,K.A. and Turner,M.S. (1982). Phys.Rev. D25,213.

Oort,J.H. (1983). Ann.Rev.Ast.Ap. 21,

Ostriker,J. and Peebles,P.J.E. (1973). Ap.J.186,467.

Pagels,H.R. and Primack,J.R. (1982). Phys.Rev.Lett. 48,223.

Peccei,R. and Quinn, H. (1977). Phys.Rev. D16,1791.

Peebles,P.J.E. (1968). Ap.J.153,1.

Peebles,P.J.E. and Dicke,R.H. (1968). Ap.J. 154,891.

Peebles,P.J.E. (1974). Ap.J.Lett. 189,L51.

Peebles,P.J.E. and Groth,E.J. (1975). Ap.J.196,1.

Peebles,P.J.E. (1976a). Ap.J.Lett. 205,109.

Peebles,P.J.E. (1976b). Ap. Space Sci. 45,3.

Peebles,P.J.E. (1980). Large scale Structure of the Universe, princeton university press,Princeton.

Peebles,P.J.E. (1981). In Xth Texas Symposium on Relativistic Astrophysics, Ann.N.Y.Acad.Sci. 375,157.

Peebles,P.J.E. (1982). Ap.J.Lett. 263,L1.

Peebles,P.J.E.: (1982b)Ap.J. 258,415.

Peebles,P.J.E. (1984).Ap.J. 277,470.

Preskill,J. et.al. (1983). Phys.Lett. 120B,127.

Peterson,S.D. (1979). Ap.J. 232,20.

Press,W.H. and Vishniac,E.T. (1980). Ap.J. 236,323.

Press,W.H. and Davis,M. (1982). Ap.J. 259,449.

Primack,J.R. and Blumenthal,G.R. (1983). In Fourth Workshop on Grand Unification H.A.Weldon et. al. (Eds.) Birkhauser,Boston; p.256.

Rees,M.J. (1971).In Proc. of the Int. School of Physics "Enrico Fermi" course 47: B.Sachs(Ed.)Gen.Rel.Cosmology Academic, N.Y.

Rees,M.J. and Ostriker,J. (1977). M.N.R.A.S. 179,541.

Rees,M.J. (1978). In Observational Cosmology,Saas-Fee, VIIIth course Geneva Observatory,Sauverny;p.259.

Reines,F. et.al. (1980). Phys.Rev.Lett. 45,1307.

Rubin,V.C. et.al. (1978). Ap.J.Lett. ,L107.

Rubin,V.C. et.al. (1982). Ap.J. 261,439.

Sandage,A. and Hardy,E. (1973). Ap.J. 183,743.

Sandage,A. and Tammann,G.A. (1981). A Revised Shapely-Ames Catalog of Bright Galaxies; Carnegie Institution, Washington.

Sargent,W.L.W. et.al. (1981). Ap.J.256,374.

Sato,H. and Takahara,F. (1981). Prog. Theor. Phys. 66,508.

Savoy,C.A. (1983). In Proc. Recontre de Moriond, Elementary Particles.

Schecter,P.L. (1976). Ap.J. 203,297.

Schramm,D. and Wagoner,R.V. (1977). Ann.Rev.Nucl.Sci. 24,37.

Schramm,D.N. and Steigman,G. (1981). Ap.J. 243,1.

Sciama,D.W. (1982). Phys.Lett. 114B,19.

Seitzer,P.O. (1983). Ph.D. dissertation, Univ. of Virginia.

Shapiro,P.L. et.al. (1983). Ap.J. 275,413.

Shapiro,P.L. (1983). In Clusters and Groups of Galaxies, F.Mardirossian et.al.(Eds.) Reidel Pub.;p.447.

Silk,J. (1968). Ap.J.151,459.

Silk,J. (1973). Ann.Rev.Ast.Ap. 11,269.

Silk,J. and Wilson,M.L. (1981). Ap.J.Lett. 244,L37.

Silk,J. (1982). In Astrophysical Cosmology, H.A.Bruck et.al. (Eds.) Pontificia Academica Scientarium; p.42.

Soneira,R.M. and Peebles,P.JE. (1978). A.J. 83,845.

Steigman,G. (1976). Ann.Rev.Ast.Ap. 14,339.

Sunyaev,R.A. and Zeldovich, Y.B. (1972). Ast. Ap. 20,189.

Symbalisty,E.M.D. and Schramm,D.N. (1981). Rep. Prog.Phys. 44,293.

Szalay,A.S. and Marx,G. (1976). Ast.Ap. 49,437.

Tamann,G.A. et.al. (1979). In Physical Cosmology, Les Houches Lectures, R;Balian et.al. (Eds.)(North-Holland).

Tarenghi,M. et.al.(1980). Ap.J. 235,724.

Toomre,A. (1977). In the Evolution of Galaxies and their Stellar Populations, B.M.Tinsley and R.B.Larson(eds.) (New Haven Yale Obs.);p.401.

Tremaine,S. and Gunn,J.E. (1979). Phys.Rev;Lett. 42,407.

Turner,E.L. (1976). Ap.J.208,20.

Turner,M.S. et.al. (1983). Phys.Lett. 125B,35.

Van den Berg (1975). Ast.Ap. 44,231.

Van den Berg (1982). P.A.S.P. 94,459.

Valdarnini,R. et.al. (1984). SISSA Preprint.

Wagoner,R.V. (1974). In IAU Symp. No. 63, M.S.Longair(Ed.)Reidel,Dodrecht.

Wassermann,I. (1981). Ap.J. 248,1.

Weinberg,S. (1972). Gravitation and Cosmology,Wiley,NewYork.

Weinberg,S. (1979). Phys.Rev.Lett. 42,850.

Weinberg,S. (1981).

Weinberg,S. (1982). In Astrophysical Cosmology,H.A.Bruck et.al. (ed.)
Pontificia Academia Scientarium,p.503.

Weinberg,S. (1983). Phys.Rev.Lett. 50,387.

Wheeler,J.A. (1957). Ann.Phys. 2,604.

White,S.D.M. (1978). M.N.R.A.S. 184,185.

White,S.D.M. et.al. (1983). Ap.J.Lett.274,L1.

Wilczek,F. (1978). Phys.Rev.Lett. 40,279.

Witten, E. (1980). Phys.Lett. 91B,81.

Witten, E. (1984). Phys. Rev. D

Yang,J. et.al. (1984). Preprint.

Zeldovich,Y.B. (1982). Nature 300,407.

Zeldovich,Y.B. (1972). M.N.R.A.S. 160,1p.

Zeldovich,Y.B. (1970). Ast.Ap. 5,84.